A DISSERTATION

ON

Performance Analysis Of Cooperative Noma System

Submitted In Partial Fulfilment of the Requirement for the Award of the Degree in

M.Tech

In

ELECTRONIC CIRCUITS AND SYSTEMS

Submitted By:

Sabra Akhtar Siddiqui

Roll No. : 2101311004

Under the Guidance of

Mr. Saif Ahmad   **Mr. Mohd Javed Khan**

(Supervisor)   **(Co-Supervisor)**

Department of Electronics & Communication Engineering

INTEGRAL UNIVERSITY, LUCKNOW-226026

June-2023

DECLARATION

This is to certify that I, Sabra Akhtar Siddiqui (Roll No.: 2101311004), have completed the M.Tech Dissertation work on topic **"Performance Analysis of Cooperative NOMA System"** under the supervision of Mr. Saif Ahmad and Mr. Mohd Javed Khan for the partial fulfillment of the requirement for the Master of Technology in Electronic Circuits and Systems from Department of Electronics and Communication Engineering, Integral University, Lucknow. This is an original piece of work & I have not submitted it earlier elsewhere.

Date: Signature

Place   Sabra Akhtar Siddiqui

                                                            Roll No.: 2101311004

CERTIFICATE

This is to certify that the dissertation titled **"Performance Analysis of Cooperative NOMA System"** has been carried out by Sabra Akhtar Siddiqui(Roll No.: 2101311004) under my supervision and guidance in partial fulfilment of the requirements for the award of degree of **"Master of Technology"** in Electronic Circuits and Systems at department of Electronics and Communication Engineering, Integral University, Lucknow, India.

<table>
<tr><td>**Mr. Saif Ahmad**</td><td>**Mr. Mohd Javed Khan**</td></tr>
<tr><td>Supervisor</td><td>Co-Supervisor</td></tr>
<tr><td>Assistant Professor</td><td>Assistant Professor</td></tr>
<tr><td>Dept. of ECE,</td><td>Dept. of ECE,</td></tr>
<tr><td>Integral University,</td><td>Integral University,</td></tr>
<tr><td>Lucknow</td><td>Lucknow</td></tr>
</table>

ACKNOWLEDGEMENT

ABSTRACT

Non-orthogonal multiple access (NOMA) is a promising technique for the fifth generation (5G) wireless communications. As users with good channel conditions can serve as relays to enhance the system performance by using successive interference cancellation (SIC), the integration of NOMA and cooperative relaying has recently attracted increasing interests.

In this dissertation, a NOMA-based cooperative relaying system is studied, and an analytical framework is developed to evaluate its performance. Specifically, the performance of NOMA over Rician fading channels is studied, and the exact expression of the average achievable rate is derived. Moreover, we also propose an approximation method to calculate the achievable rate by using the Gauss–Chebyshev Integration. Numerical results confirm that our derived analytical results match well with the Monte Carlo simulations.

LIST OF CONTENTS

Chapter	Particulars	PAGE No.

LIST OF FIGURE

SYMBOLS AND ABBREVIATIONS

SINR	Signal-to interference-plus-noise ratio
AWGNs	Additive White Gaussian Noises
CDF	Cumulative Distribution Function
R	Bit rate
B	Bandwidth
CR	Cognitive Radio
DSP	digital signal processing
AWGN	additive white Gaussian noise
PDF	Probability density function
CSI	Channel State Information
QoS	Quality of service
AF	Energy efficiency
DF	Decode-and-Forward
BS	Base Station
NOMA	Non-Orthogonal Multiple Access
OMA	Orthogonal Multiple Access
Ops	Outage Probabilities
RX	Receiver
N₀	noise power spectral density
B	Bandwidth
SIC	Successive Interference Cancellation
SNR	Signal to Noise Ratio
SOPs	Secrecy Outage Probabilities
TX	Transmitter

Chapter 1

INTRODUCTION

It is highly expected that future 5G networks should achieve a 10-fold increase in connection density, i.e., 10^6 connections per square kilometers [1]. Non-orthogonal multiple access (NOMA) has been proposed as a promising candidate to realize such an aggressive 5G goal [2]–[5]. NOMA is fundamentally different from conventional orthogonal multiple access (OMA) schemes such as FDMA, TDMA, OFDMA, etc., since it allows multiple users to simultaneously transmit signals using the same time/frequency radio resources but different power levels [3]–[5]. The key advantage of NOMA is to explore the extra power domain to further increase the number of supportable users. Specifically, users are identified by their channel conditions, those with good channel conditions are called strong users and others are called weak users. For the sake of fairness, less power are allocated to strong users at the transmitter side. In this way, the transmitter sends the superposition of signals with different power levels and the receiver applies successive interference cancellation (SIC) to strong users to realize multi-user detection [5], [6]. Such non-orthogonal resource allocation enables NOMA to accommodate more users and makes it promising to address the 5G requirement of massive connectivity, with the cost of controllable increase of complexity in receiver design due to SIC [5].In NOMA systems, the use of SIC implies that strong users have prior information about the messages of other users, so essentially they are able to serve as cooperative relays. Moreover, cooperative relaying is able to significantly enhance the system performance of cellular networks [7]. Thus, combining cooperative relaying and NOMA is promising to improve the throughput of future 5G wireless networks, and has attracted increasing interests recently [8]. Specifically, a cooperative NOMA transmission scheme was proposed in [9], where strong users decode the signals that are intended to others and serve as relays to improve the performance of weak users. Another NOMA-based cooperative scheme was proposed in [10], where the performance of a NOMA-based decode-and-forward relaying system under Rayleigh fading channel was studied. However, most of existing NOMA schemes only consider the Rayleigh fading channel, which is suitable for rich scattering scenarios without line of sight (LOS), while little attention has been drawn to the more general Rician fading channel, which takes both LOS and non LOS (NLOS) into consideration.

In some typical 5G application scenarios, such as massive machine-type communications (mMTC) and Internet of things (IoT), "users" may be low-cost sensors deployed in a small area, where both LOS and NLOS exist, which can be better modeled by the Rician fading channel. In this paper, we investigate the performance of the NOMA-based cooperative relaying transmission scheme in [10] under Rician fading channels1 Evaluating system performance under Rician fading channel is rather challenging as the probability density function of Rician distribution variables consists of Bessel function, which makes it difficult to calculate the average achievable rate through integration. In order to derive the exact expression of the achievable rate, we propose an analytical method using Taylor expansion of Bessel function and incomplete Gamma function. However, the complexity of the incomplete Gamma function makes it still difficult to get the exact values, so we further propose an approximation method using Gauss-Chebyshev Integration to simplify the calculation. Finally, simulations confirm that our analytical results match well with the Monte Carlo results.

Comparing with wired communication, the wireless network has been the practical communication method due to its convenience and flexibility in varies environments. In conjunction with the development of the beyond fifth-generation (5G) and sixth-generation (6G) mobile communications, various kinds of Internet of Things (IoT) devices (e.g., smartphones, smart watches and other IoT sensors) are designed and produced. The number of these devices is predicted to keep increasing in the upcoming years. Therefore, connecting massive number of devices through wireless signals will become more important. The most critical challenge for wireless systems is to find practical solutions in performance and secrecy improvement, i.e., to achieve reliable transmission and keep the information safe while improving data rates as well as confidentiality.

To cope with the above challenge, in this dissertation, a cooperative network technology is focused on, and the modern technologies to the emerging wireless scenarios is applied. In this chapter, we will review these advanced schemes.

1.1 Backgrounds

1.1.1 Cooperative Networks

Cooperative communication is widely considered as a means to make the transmitting signals

robust against fading environment, to compensate for the power limitation in the wireless communication devices, and therefore to improve the range of wireless communication [1–5]. A concept of a most widely studied cooperative network is illustrated in Fig. 1.1, where two nodes communicate with the same destination. Since each wireless node is equipped with a single antenna, and thus its spatial diversity cannot be achieved. During the long-distance transmission in a fading environment, or if the building and other obstacles block the direct link, the other nodes help the source nodes as relay. Among many cooperative relaying protocols, the most wildly investigated are the amplify-and-forward (AF) protocol and the decode-and-forward
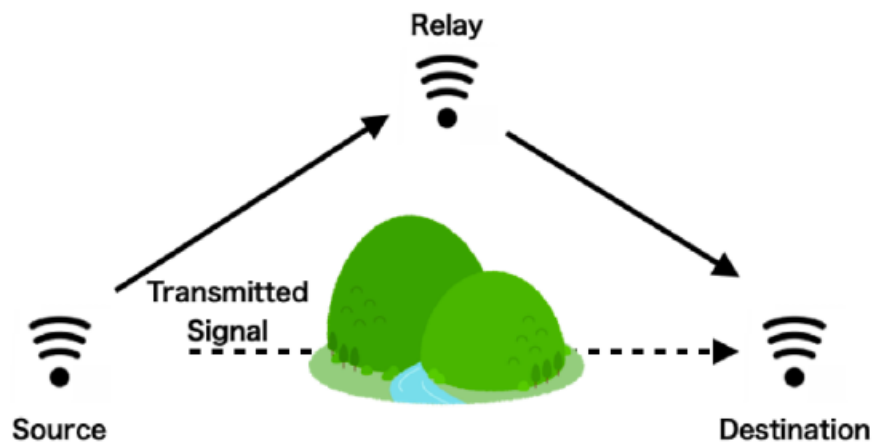

Figure 1.1: Fundamental illustration of cooperative relaying networks

(DF) protocol [6,7]. In AF protocol, relay amplifies the received data from source without decode and re-encode process, then transmits it to destination [8–15]; In DF protocol, the relay first decodes the received signal before the forwarding process [16–23]. In this dissertation, we are interested in the DF protocol.

1.1.2 Unmanned Aerial Vehicle (UAV) Communication

Unmanned aerial vehicle (UAV) enabled systems and their wireless communication networks are considered for a variety of applications, such as security operations in the military, entertainment, and telecommunications in recent decades [24–30]. The number of UAV applications is increasing in the telecommunication industry, e.g., relay-base stations (BSs), communication gateways, data collection in wireless sensor networks, search and rescue operations in earthquake area, entertainment industry, and power lines maintenance [31]. The

potential role of UAVs as a relay BS in hotspots, congested area, makes them an inherent part of the next-generation communication infrastructure [32].

1.1.3 NOMA Technology

In order to achieve enhanced spectrum efficiency of the wireless mobile network, non orthogonal multiple access (NOMA) has received attention by the researchers focusing on wireless systems [40–42]. Notably, different devices can share the same time and frequency spectrum with cooperative power allocation adjustment. Through the use of successive interference cancellation (SIC), the devices with weak power conditions can decode its own information after removing those strong power condition [43, 44], which has been investigated as an extension of the network-assisted interference cancellation and suppression (NAICS) in 3GPP [45, 46].

This technique significantly improve the spectral efficiency and outperform traditional orthogonal multiple access (OMA) schemes under the limitation of frequency spectrum. In Fig. 1.2, we illustrate the difference between OMA and NOMA. The OMA technique contains orthogonal frequency division multiple access (OFDMA) or time division multiple access (TDMA). In OFDMA, multiple devices are allocated with orthogonal subcarriers contacted via the orthogonal frequency-division multiplexing (OFDM) technique. In TDMA, the devices divide the signal into different time slots in order to share the same frequency channel. The downlink scenario with NOMA scheme is demonstrated in Fig. 1.2(a), where two devices (i.e., U1 and U2) receive information from a single base station (BS) with the same transmission channel. The BS continuously sends the signal to U1 and U2 simultaneously, where the two different signals are non-orthogonally superposed. In the decoding process, U1 needs to decode the signal of U2 and run SIC process of U2 signal before decoding its own signal.

(a) NOMA

(b) OMA

Figure 1.2: Multiple access scenarios for two devices that form a pair

this dissertation, we apply the NOMA technology in UAV-aided model in order to improve the transmission performance of the wireless communication system.

1.1.4 Physical Layer Security

Exchanging information over wireless channels is vulnerable to eavesdropping attacks and jamming attacks from malicious nodes due to the broadcast nature of wireless communications. In recent years, the critical issue of security against eavesdropper attacks is widely investigated in the different types of wireless networks [47–49]. In order to protect from wireless information leakage, cryptography-based secrecy methods are widely utilized in the upper layer of various

wireless transmission protocols. Cryptography-based systems encrypt information with various secret key generation protocols. In most research assumptions, eavesdroppers could not decrypt the wiretapped signal in a limited time through exhaustive search due to the limitation of computing capabilities. Nevertheless, the computing capabilities of eavesdroppers increase significantly in recent years. These traditional cryptography-based solutions are facing a critical risk of being broken via the relentless brute-force attacks of eavesdropper with a short period [50, 51]. Furthermore, in the wireless distributed networks, the decentralized framework of the network design makes the secret keys difficult to be managed and distributed. This requires the introduction of more powerful secrecy methods to increase the security of wireless networks and decrease the method complexity. Therefore, physical layer (PHY) security methods have been proposed in order to provide effective security assurance for wireless networks [52]. Compared to cryptography-based solutions, PHY security has several obvious advantages. It can guarantee information secrecy regardless of the computational capabilities of eavesdroppers. The costly centralized secret key management/distribution methods, which are widely used in cryptography based security systems, could be eliminated in PHY security techniques, which facilitated the management and improving the efficiency of wireless communication networks.

The PHY security dates back to Wyner's wiretap model [53]. Wyner's results show that without using any secret key protocols between the legitimate transmitter-receiver pairs, the nonzero secrecy rate can be achieved. In the extension researches of Wyner's problem, the secrecy capacity is defined as the difference between Shannon's capacities of the main and eavesdropper channels [54, 55]. In order to improve the secrecy rate, PHY security techniques have been developed based on the inherent randomness of both the main and eavesdropper channels of wireless networks. In this dissertation, we focus on the following schemes:

• **Cooperative Jamming:** Cooperative jamming allows the idle nodes to send artificial noise (AN) to eavesdroppers for the secrecy capacity improvement of a given transmitter receiver pair [56–59]. AN is usually assumed as a random generated noise with Gaussian distribution independent of the intended information signal, which helps to degrade the information received at the eavesdropper [56]. Particularly, AN used for jamming could be structured by some specific code words that can be canceled only at legitimate devices [58].

Even though no channel state information (CSI) about the eavesdropper channel is needed in the cooperative jamming scheme, the interference that caused by AN could also degrade the transmission performance of the main channel due to the interference.

• **Relay Selection:** In order to enlarge the secrecy capacity between the main and eaves dropper channels, the relay selection strategy could improve the secrecy performance by choosing a robust main link but a weak eavesdropper link [60–63]. The selected relay should transmit information in a prefixed manner without considering the current channel quality. In order to address this limitation, buffer-aided relay selection strategies have been proposed, where relays select the best link from all available links to transmit buffer stored delay-tolerant information based on the current channel gains [62, 63]. Even though relay selection will not decrease the performance of transmissions in the main channel, the full CSI of the eavesdropper channel is always required due to the optimized relay selection strategy, which may not be practical in the realistic scenario.

• **Beamforming and Precoding:** Beamforming is the technology that transmits one data stream through multiple antennas by adjusting the signal phase [64–67]. The direction of the antennas and the phase alignment of signals are controlled by the controller unit of the transmitter such that the antenna matrix at the transmitter concentrates the signal strength towards the direction of the intended receiver. In contrast, the signal strength is maximized at the eavesdropper should be limited. However, precise synchronization between the transmitter and receiver is required. It also requires the perfect knowledge of eavesdropper CSI for beamforming. AN in order to prevent information leakage.

1.1.5 Wireless Power Transfer (WPT)

In the modern wireless network, the cooperative communication is proposed with the help of intermediate cooperative nodes that forward the information of the source to the destination in a long-distance transmission scenario. The cooperative relay nodes could be subject to severe energy limitation during the long time transmission due to the battery capacity [68, 69]. A radiofrequency (RF) wireless power transfer (WPT) offers an available option to extend the lifetime of low energy-level cost wireless networks with such external power sources. The receiver could extend its lifetime by receiving RF signal for energy recharging. Moreover, transmitting sufficient power to the low-power IoT devices is possible by WPT system. For

instance, a distributed WPT system was proposed for wireless charging of low power IoT devices in [70].

2.1 Fading Channel Models

In a wireless system, the signal will interact with highly complex environment before it is received by the receiver, such as Doppler shift, and fading. In this dissertation, the transmission processes consist of discrete-time blocks in short time is assumed. The channel gain is non-frequency selective and constant in each block and independent and identically distributed, i.e., block fading [71]. As the statistical result based on measurements, if there are only scattered paths between the transmitter and receiver (also called non line-of-sight (NLOS) scenario), the channel gain follows zero-mean circularly symmetric Gaussian distribution. Hence, the signal envelope follows Rayleigh distribution, with its probability density function (PDF) as [71, (3.32)]

$$f_z^{Rayleigh}(z) = \frac{z}{\sigma^2} \exp\left(-\frac{z^2}{2\sigma^2}\right) \quad (1.1)$$

where σ^2 is the second moment of random variable Z. Conversely, if the channel consists of both direct path (also called line-of-sight (LoS) component) and scattered paths, the channel gain follows non zero-mean circularly symmetric Gaussian distribution. Hence, the signal envelope in such case can be shown to have Rician distribution with its PDF as [71, (3.37)]

$$f_z^{Rician}(z) = \frac{2(K+1)z}{\Omega} e^{-\left(k + \frac{(k+1)z^2}{\Omega}\right)} I_0\left(2\sqrt{\frac{k(k+1)}{\Omega}} z\right) \quad (1.2)$$

where K is defined as the ratio between the power in direct path components and scattered multipath components, Ω is defined as the total power received from paths, and $I_0(\cdot)$ is the zero-ordered modified Bessel function of first kind. For special cases, while K = 0, Rician distribution will degrade to Rayleigh distribution; while K = ∞, the channel will have no fading, i.e., additive white Gaussian noise (AWGN) channel.

Furthermore, in order to simplify the numerical evaluation of Rician fading channel, Nakagami-m fading model is often adopted to approximate the Rician fading, where the PDF is expressed in closed-form as [71, (3.38)].

$$f_z^{Nakagami}(z) = \frac{2m^m z^{2m-1}}{\Gamma(m)\Omega^m} z^{2m-1} \exp\left(-\frac{m}{\Omega}z^2\right) \quad (1.3)$$

with parameter $m \triangleq (K+1)^2/(2K+1)$, and Ω follows the same definition as Rician distribution. For special cases, if $m = 1$ the distribution reduces to Rayleigh fading; while $m = \infty$, the channel is approximately equal to AWGN channel.

Chapter 2

Literature Survey

.

Federico Boccardi et al. (2014) described the five disruptive research directions that could lead to fundamental changes in the design of cellular networks. We have focused on technologies that could lead to both architectural and component design changes: device-centric architectures, mm Wave, massive MIMO, smarter devices, and native support of M2M. It is likely that a suite of these solutions will form the basis of 5G.

Linglong Dai et al. (2018) discussed the key concept and advantages of NOMA techniques, which constitute one of the promising technologies for future 5G systems. The dominant NOMA schemes have been introduced together with their comparison in terms of their operating principles, key features, receiver complexity, pros and cons, etc. We also highlighted a range of key challenges, opportunities and future research trends related to the design of NOMA, including the theoretical analysis, the design of spreading sequences or codebooks, the receiver design, the design issues of access-grant-free NOMA, resource allocation schemes, extensions to massive MIMO systems and so on. It is expected that NOMA will play an important role in future 5G wireless communication systems supporting massive connectivity and low latency.

Fang Fang et al. (2016) discussed the assigning only two users to the same sub channel, we proposed energy-efficient resource allocation algorithms for a downlink NOMA wireless network. These algorithms include sub channel assignment, power proportional factors determination for multiplexed users and power allocation across sub channels. By formulating sub channel assignment problem as a two-sided matching problem, we proposed the SOMSA algorithm to maximize the system energy efficiency. Power proportional factors for the multiplexed users on each sub channel are determined by SOMSA. In the power allocation across sub channels scheme, since the objective function is non convex, DC programming was utilized to approximate the non convex optimization problem into the convex sub-problem. Therefore, a suboptimal power allocation across sub channels was obtained by solving the convex sub-problems iteratively. Based on the resource scheduling from proposed SOMSA algorithm, further improvement in the system energy efficiency was achieved by the proposed sub channel power allocation scheme. Through extensive simulations, the performance of the

proposed algorithms for resource allocation was compared with the OFDMA system. It was shown that the total sum rate and energy efficiency of NOMA system are much higher than the OFDMA scheme. The proposed power allocation for subchannel users outperforms the FTPA scheme. Moreover, the proposed subchannel power allocation achieves better performance than the equal power allocation scheme.

Yan Sun et al. (2017) discussed the resource allocation algorithm design for an MC-NOMA system with an FD BS. The algorithm design was formulated as a mixed combinatorial non-convex optimization problem for the maximization of the weighted sum throughput of the system. Monotonic optimization was applied for solving the proposed optimization problem optimally. The resulting optimal power and subcarrier allocation policy served as a performance benchmark due to its high computational complexity. Therefore, a suboptimal algorithm based on successive convex approximation was also proposed to strike a balance between computational complexity and optimality. Simulation results showed that the proposed suboptimal algorithm obtained a close-to-optimal performance in a small number of iterations. In addition, our results revealed that a substantial improvement of system throughput can be achieved by employing the proposed FD MC-NOMA scheme compared to baseline schemes employing FD MCOMA, HD MC-NOMA, and HD MC-OMA. Furthermore, the proposed FD MC-NOMA scheme was shown to provide a good balance between improving the system throughput and maintaining fairness among users.

Yuya Saito et al. (2013) discussed the system-level performance of NOMA taking into account more practical aspects of the cellular system and some of the key parameters and functionalities of the LTE radio interface such as frequency-domain scheduling, AMC, HARQ and OLLA, in addition to NOMA specific functionalities such as dynamic multi-user power allocation. Using computer simulations, we showed that the overall cell throughput, cell-edge user throughput, and the degree of proportional fairness of NOMA are all superior to that for OMA. This is because NOMA has more degrees of freedom to co-schedule more users in the same subband. However, the order of the gains depends on multiple factors such as the number of UEs per cell and the number of sub bands for scheduling. In particular, wideband MCS selection is seen as a limiting factor to harnessing the benefits of sub band user multiplexing for NOMA. It was also found that OLLA also improves the overall cell throughput and cell-edge user throughput of NOMA, even

when dynamic power allocation is applied. Further optimizations of dynamic transmit power allocation and MCS adaptation for NOMA require further study.

Lei Liu et al. (2019) analyzes the achievable rate region of the iterative LMMSE multi-user detection for both symmetric and asymmetric MIMO-NOMA. For the symmetric case, it is proved that iterative LMMSE detection achieves the capacity of MIMO-NOMA with any number of users; while for the asymmetric case, it is proved that the iterative LMMSE detection achieves the sum capacity of MIMONOMA with any number of users. In addition, all the maximal extreme points in the capacity region of MIMO-NOMA with any number of users are achievable, and all points in the capacity regions of two-user and three-user systems are also achievable. Finally, a kind of IRA multiuser code is designed for the iterative LMMSE receiver. Simulation results show that under different channel loads, the BERs of the proposed iterative LMMSE detection are within 0.8dB from the Shannon limits and outperform the existing methods. Furthermore, the improvement is more notable for large system overloads (e.g. $\beta \geq 3$), while for small system overloads (e.g. $\beta \leq 0.5$), the AWGN SU-IRA and the MMSE SIC with SU-IRA is good enough since the user interference is negligible.

J. Nicholas Laneman et al.(2004) develop a variety of low-complexity, cooperative protocols that enable a pair of wireless terminals, each with a single antenna, to fully exploit spatial diversity in the channel. These protocols blend different fixed relaying modes, specifically amplify-and-forward and decode-and-forward, with strategies based upon adapting to CSI between cooperating source terminals (selection relaying) as well as exploiting limited feedback from the destination terminal (incremental relaying). For delay-limited and nonergodic environments, we analyze the outage probability performance, in many cases exactly, and in all cases using accurate, high-SNR approximations.

Yuanwei Liu et al. (2016) the application of SWIPT to NOMA has been considered. A novel cooperative SWIPT NOMA protocol with three different user selection criteria has been proposed. We have used the stochastic geometric approach to provide a complete framework to model the locations of users and evaluate the performance of the proposed user selection schemes. Closed-form results have been derived in terms of outage probability and delay-sensitive throughput to determine the system performance. The diversity gain of the three user selection schemes has also been characterized and proved to be the same as that of a conventional cooperative network. For the proposed protocol, the decreasing rate of the outage

probability of far users is $\left(\frac{\ln\text{SNR}}{\text{SNR}^2}\right)$ while it is $\left(\frac{1}{\text{SNR}^2}\right)$ for a conventional cooperative network. Numerical results have been presented to validate our analysis. We conclude that by carefully choosing the parameters of the network, (e.g. transmission rate or power splitting coefficient), acceptable system performance can be guaranteed even if the users do not use their own batteries to power the relay transmission.

Zhiguo Ding et al. (2015) discussed a proposed a cooperative NOMA transmission scheme which uses the fact that some users in NOMA systems have prior information about the others' messages. Analytical results have been developed to demonstrate the performance gain of this cooperative NOMA scheme. Fixed choices of power allocation coefficients have been used in this paper, and it is important to study optimal power allocation for cooperative NOMA [8], [9]. Another promising future direction is to apply simultaneous wireless information and power transfer to NOMA in order to alleviate practical constraints.

Jung-Bin Kim et al. (2015) discussed the proposed the CRS using NOMA, and presented the exact and asymptotic expressions for the achievable average rate of the proposed system in independent Rayleigh fading channels. In addition, we presented the suboptimal power allocation scheme for NOMA that provides almost the same performance as the optimal power allocation for high SNR. The proposed CRS using NOMA can achieve more spectral efficiency than the conventional CRS when the SNR is high and the average channel power of the S-to-R link is better than those of the S-to-D and R-to-D links.

Manav R. Bhatnagar (2013) In this paper described the probability density function (PDF) and cumulative distribution function (CDF) of the minimum of two non-central Chi-square random variables with two degrees of freedom in terms of power series. With the help of the derived PDF and CDF, we obtain the exact ergodic capacity of the following adaptive protocols in a decode-and forward (DF) cooperative system over dissimilar Rician fading channels: (i) constant power with optimal rate adaptation; (ii) optimal simultaneous power and rate adaptation; (iii) channel inversion with fixed rate. By using the analytical expressions of the capacity, it is observed that the optimal power and rate adaptation provides better capacity than the optimal rate adaptation with constant power from low to moderate signal to-noise ratio values over dissimilar Rician fading channels. Despite low complexity, the channel inversion based adaptive transmission is shown to suffer from significant loss in capacity as compared to the other adaptive transmission based techniques over DF Rician channels.

Ali Abdi et al. (2001). In this paper we have studied the statistical behavior of two moment-based estimators for the parameter of Rice fading distribution, as simple alternatives to the more complex maximum likelihood estimator. We have shown, analytically, that there is a tradeoff between the simplicity and the efficiency of these two estimators. The normalized asymptotic variance of the more complex estimator is very close to the Cramer–Rao lower bound, whereas for the simpler estimator, the normalized asymptotic variance deviates from the Cramer–Rao lower bound, slightly. The effect of finite sample size is also investigated via Monte Carlo simulation. Moreover, we have analyzed the impact of fading correlation on the performance of the two estimators. Our results suggest that for low mobile speed (small Doppler spread), which introduces significant correlation among signal samples, the estimators' performance becomes deteriorated due to the reduction in the number of independent samples. In summary, the simpler estimator, which shows a good compromise between computational convenience and statistical efficiency, could be recommended for practical applications.

E. Tekin and A. Yener (2008) In this paper, we have considered the Gaussian multiple-access and two-way channels in the presence of an external eavesdropper who receives the transmitted signals through a multiple-access channel, and provided achievable secrecy rates. We have shown that the multiple-access nature of the channels considered can be utilized to improve the secrecy of the system. In particular, we have shown that the total extra randomness is what matters mainly concerning the eavesdropper, rather than the individual randomness in the codes. As such, it may be possible for users whose single-user wiretap capacity are zero, to communicate with nonzero secrecy rate, as long as it is possible to put the eavesdropper at an overall disadvantage. This is even clearer for two-way channels, where even though the eavesdropper's channel gain may be better than a terminal's, the extra knowledge of its own codeword by that terminal enables communication in perfect secrecy as long as the eavesdropper's received signal is not strong enough to allow single-user decoding. We found achievable secrecy rate regions for the GGMAC-WT and the GTW-WT. We also showed that for the GGMAC-WT the secrecy sum rate is maximized when only users with "strong" channels to the intended receiver as opposed to the eavesdropper transmit, and they do so using all their available power. For the GTW-WT, the sum rate is maximized when both terminals transmit with maximum power as long as the eavesdropper's channel is not good enough to decode them using single-user decoding. Finally, we proposed a scheme termed cooperative jamming, where a

disadvantaged user may help improve the secrecy rate by jamming the eavesdropper. We found the optimum power allocations for the transmitting and jamming users, and we showed that significant rate gains may be achieved, especially when the eavesdropper has much higher SNR than the receivers and normal secret communications is not possible. The gains can be significant for both the GGMAC-WT and the GTW-WT. This cooperative behavior is useful when the maximum secrecy sum rate is of interest. We have also contrasted the secrecy rates of the two channels we considered, noting the benefit of the two-way channels where the fact that each receiver has perfect knowledge of its transmitted signal brings an advantage with each user effectively encrypting the communications of the other user. In this paper, we only presented achievable secrecy rates for the GGMAC-WT and the GTW-WT. The secrecy capacity region for these channels are still open problems. In [45], we also found an upper bound for the secrecy sum rate of the GGMAC-WT and noted that the achievable secrecy sum rate and the upper bound we found only coincide for the degraded case, so that we have the secrecy sum capacity for the degraded GMAC-WT. Even though there is a gap between the achievable secrecy sum rates and upper bounds, cooperative jamming was shown in [45] to give a secrecy sum rate that is close to the upper bound in general. Finally, we note that the results provided are of mainly theoretical interest, since as of yet there are no currently known practical codes for multiple-access wiretap channels unlike the single-user case where in some cases practical codes have been shown to be useful for the wiretap channel [46], [47]. Furthermore, accurate estimates of the eavesdropper channel parameters are required for code design for wiretap channels where the channel model is quasi-static, as in our models considered in this paper.

CHAPTER 3

Mathematical Modeling of NOMA-based cooperative relaying system

3.1 SYSTEM MODEL:

The system model of the NOMA-based cooperative relaying system is introduced in this chapter. .We consider a simple cooperative relaying system (CRS) consisting of a source (S), decode-and-forward relay (R) which works in half-duplex mode, and a destination (D).We assume that all links between them (i.e., S-to-D, S to-R, and R-to-D) are available. The independent Rician fading channel coefficients of S-to-D, S-to-R, and R-to-D links are denoted as g_{SD}, g_{SR}, and g_{RD}, with the average powers of ω_{SD}, ω_{SR}, and ω_{RD}, respectively. It is also assumed that $\omega_{SD} < \omega_{SR}$, since in general the path loss of the S-to-D link is usually worse than that of the S-to-R link [10]. In the traditional CRS presented in Fig. 3.1(a), the source transmits s_1 to the relay and destination in the first time slot. Then in the second time slot, the relay transmits s_2 to the destination. In this way, the destination only receives one signal in two time slots. In the NOMA-based CRS showed in Fig. 3.1(b), the destination is able to receive two different signals in two time slots, so it outperforms the traditional CRS in terms of throughput. Specifically, in the first time slot, the source transmits the superposition of two different data symbols s1 and s2 to the relay and the destination as follows:
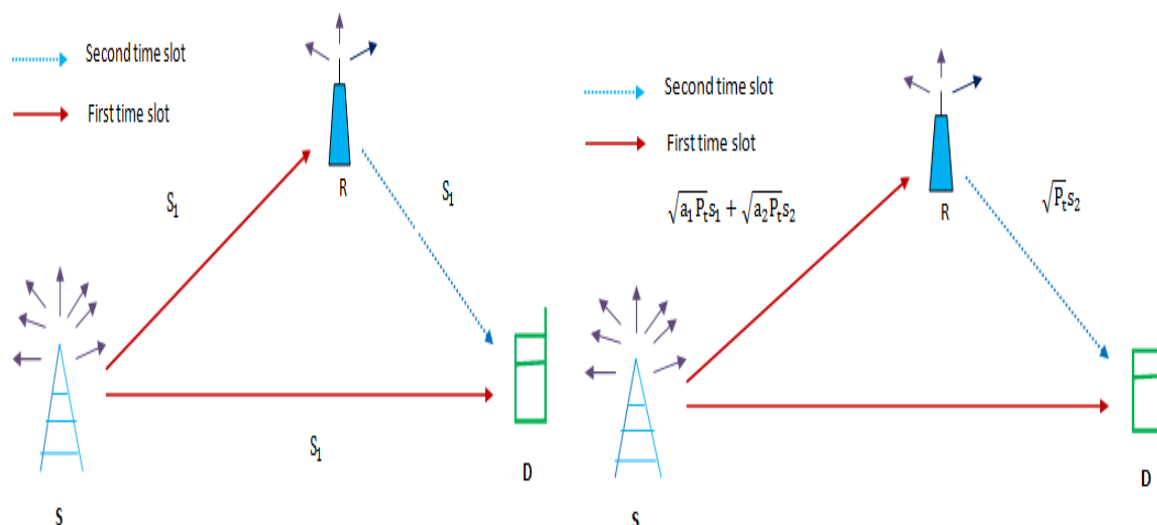

Fig.3.1. System models of two cooperative relaying systems: (a) Traditional cooperative relaying systems; (b) NOMA-based cooperative relaying systems.

$$y = \sqrt{a_1 P_t} s_1 + \sqrt{a_2 P_t} x s_2 \tag{3.1}$$

where s_i denotes the i-th data symbol with normalized power $E[|s_i|^2] = 1$, S_t is the total transmit power, and a_i is the power allocation coefficient. It is noted that $a_1 + a_2 = 1$, and $a_1 > a_2$ due to $\Omega_{SD}^2 < \Omega_{SR}^2$ [5]. Thus, the received signals r_{SR} and r_{SD} at the relay and the destination in the first time slot are respectively expressed as

$$r_{SR} = h_{SR} \left(\sqrt{a_1 P_t} s_1 + \sqrt{a_2 P_t} s_2 \right) + n_{SR} \tag{3.2}$$

$$r_{SD} = h_{SD} \left(\sqrt{a_1 P_t} s_1 + \sqrt{a_2 P_t} s_2 \right) + n_{SD} \tag{3.3}$$

where n_{SR} and n_{SD} denote the additive white Gaussian noise (AWGN) with zero mean and variance σ^2. The destination only decodes symbol s_1 by treating symbol s_2 as noise, while the relay acquires symbol s_2 from (1) using SIC. Thus, the received signal-to-interference plus noise ratios (SINRs) for symbols s and s_2 at the relay can be respectively obtained as

$$\gamma_{SR}^1 = \frac{|h_{SR}|^2 a_1 P_t}{|h_{SR}|^2 a_1 P_t + \sigma^2} \tag{3.4}$$

$$\gamma_{SR}^2 = \frac{|h_{SR}|^2 a_2 P_t}{\sigma^2} \tag{3.5}$$

and the received SINR for symbol s_1 at the destination is obtained as

$$\gamma_{SD} = \frac{|h_{SD}|^2 a_1 P_t}{|h_{SD}|^2 a_1 P_t + \sigma^2} \tag{3.6}$$

perfectly decode symbol s_2 in the first time slot [5], the received signal at the destination in the second time slot can be expressed as

$$r_{RD} = h_{RD} \sqrt{P_t} x_2 + n_{RD} \tag{3.7}$$

where n_{RD} is the AWGN with zero mean and variance σ^2, and the received SINR for symbol s_2 in (3.7) can be obtained as

$$\gamma_{RD} = \frac{|h_{RD}|^2 P_t}{\sigma^2} \tag{3.8}$$

As the expressions for received signals and SINRs are already acquired, we will calculate both the exact and approximated achievable rates in the NOMA-based CRS in the next section.

In this chapter, we first derive the exact expression of the average achievable rate of the NOMA-based CRS over Rician fading channel. As the exact value of achievable rates are difficult to calculate, we further propose an approximation method using Gauss-Chebyshev Integration to simplify the numerical calculation.

3.2 Achievable Rate Analysis :

In this subsection, we analyze the average achievable rate of s_1 and s_2. Let $\lambda_{SD} \triangleq |h_{SD}|^2$, $\lambda_{SR} \triangleq |h_{SR}|^2$, $\lambda_{RD} \triangleq |h_{RD}|^2$ and $\triangleq \frac{P_t}{\sigma^2}$, where ρ represents the transmit SNR. As both the relay and the destination must successfully decode s_1 and s_2, the rates of these two signals should be lower than the rates of both links calculated by Shannon formula, so the achievable rate is the minimum of the rates of two different links. According to [10], we can obtain the achievable rates C_{s_1} and C_{s_2} of signals s_1 and s_2 respectively as

$$C_{s_1} = \frac{1}{2} \min\{\log_2(1 + \gamma_{SD}), \log_2(1 + \gamma_{SR}^1)\} \tag{3.9}$$

$$C_{s_1} = \frac{1}{2} \log_2[1 + \min\{\gamma_{SR}^1, \gamma_{SD}\}] \tag{3.10}$$

$$C_{s_1} = \frac{1}{2} \log_2\left[1 + \min\left\{\frac{|h_{SR}|^2 a_1 P_t}{|h_{SR}|^2 a_2 P_t + N_0}, \frac{|h_{SD}|^2 a_1 P_t}{|h_{SD}|^2 a_2 P_t + N_0}\right\}\right] \tag{3.11}$$

$$C_{s_1} = \frac{1}{2} \log_2\left[1 + \min\left\{\frac{\lambda_{SR} a_1 \rho_1}{\lambda_{SR} a_2 \rho_1 + 1}, \frac{\lambda_{SD} a_1 \rho_1}{\lambda_{SD} a_2 \rho_1 + 1}\right\}\right] \tag{3.12}$$

$$C_{s_1} = \frac{1}{2} \log_2\left[1 + \frac{\min\{\lambda_{SR}, \lambda_{SD}\} a_1 \rho_1}{\min\{\lambda_{SR}, \lambda_{SD}\} a_2 \rho_1 + 1}\right] \tag{3.13}$$

$$C_{s_1} = \frac{1}{2} log_2 \left[\frac{\min\{\lambda_{SR}, \lambda_{SD}\} a_2 \rho_1 + 1 + \min\{\lambda_{SR}, \lambda_{SD}\} a_1 \rho_1}{\min\{\lambda_{SR}, \lambda_{SD}\} a_2 \rho_1 + 1} \right] \quad (3.14)$$

$$C_{s_1} = \frac{1}{2} log_2 \left[\frac{\min\{\lambda_{SR}, \lambda_{SD}\} a_2 \rho_1 + \min\{\lambda_{SR}, \lambda_{SD}\} a_1 \rho_1 + 1}{\min\{\lambda_{SR}, \lambda_{SD}\} a_2 \rho_1 + 1} \right] \quad (3.15)$$

$$C_{s_1} = \frac{1}{2} log_2 \left[\frac{\min\{\lambda_{SR}, \lambda_{SD}\} \rho_1 (a_1 + a_2) + 1}{\min\{\lambda_{SR}, \lambda_{SD}\} a_2 \rho_1 + 1} \right] \quad (3.16)$$

Where a_1 and a_2 are allocation of power coefficient and its value is $a_1 + a_2 = 1$ then,

$$C_{s_1} = \frac{1}{2} log_2 \left[\frac{\min\{\lambda_{SR}, \lambda_{SD}\} \rho_1 + 1}{\min\{\lambda_{SR}, \lambda_{SD}\} a_2 \rho_1 + 1} \right] \quad (3.17)$$

$$= \frac{1}{2} log_2 [1 + \min\{\lambda_{SR}, \lambda_{SD}\} \rho_1] - \frac{1}{2} log_2 [1 + \min\{\lambda_{SR}, \lambda_{SD}\} \rho_1 a_2] \quad (3.18)$$

$$C_{s_2} = \frac{1}{2} min[log_2\{1 + \gamma_{SR}^2\}, log_2\{1 + \gamma_{RD}\}] \quad (3.19)$$

$$C_{s_2} = \frac{1}{2} log_2 [1 + \min \left\{ \frac{|h_{SR}|^2 a_2 W_t}{N_0}, \frac{|h_{RD}|^2 W_t}{N_0} \right\}] \quad (3.20)$$

$$C_{s_2} = \frac{1}{2} log_2 [1 + \min\{\rho_1 a_2 \lambda_{SR}, \lambda_{RD} \rho_1\}] \quad (3.21)$$

$$= \frac{1}{2} log_2 [1 + \min\{a_2 \lambda_{SR}, \lambda_{RD}\} \rho_1] \quad (3.22)$$

To find the sum rate of messages of the DF-Relaying cooperative system using NOMA, add the equations (3.16) and (3.22)

$$C_{sum\ rate} = C_{s_1} + C_{s_2} \quad (3.23)$$

The PDF of rician fading channel can be represented as [15]

$$f_x(x) = \frac{(1 + K_x) e^{-K_x}}{\omega_x} e^{-\left(\frac{1 + K_x}{\omega_x}\right)x} I_0 \left(2 \sqrt{\frac{K_x(1 + K_x)x}{\omega_x}} \right) (x)^n \quad (3.24)$$

Where $A_x = \frac{(1+K_x)e^{-K_x}}{\omega_x}$, $a_x = (1+K_x)/\omega_x$, $B_x(n) = \frac{K_x^{n_1}(1+K_x)^n}{(\omega_x^{n_1}(n!)^2)}$ and $I_0(x) =$

$\sum_{n=0}^{\infty} \frac{(x)^{2n}}{(2)^{2n}(n!)^2}$ [17], again we written the equation(3.24) as follows:

$$f_x(x) = \frac{(1+K_x)e^{-K_x}}{\omega_x} e^{-(\frac{1+K_x}{\omega_x})x} \sum_{n=0}^{\infty} \frac{K_x^n(1+K_x)^n}{(\omega_x^n(n!)^2)}(x)^n \tag{3.25}$$

$$f_x(x) = A_x e^{-a_x x} \sum_{n=0}^{\infty} B_x(n)(x)^n \tag{3.26}$$

Let us consider $z_1 \triangleq min\{\lambda_{SR}, \lambda_{SD}\}$, $z_2 \triangleq min\{a_2\lambda_{SR}, \lambda_{RD}\}\rho_1$. We can find the CDF of z_1 using [11]

$$F(z_1) = 1 - \int_{z_1}^{\infty} f_x(x)dx \times \int_{z_1}^{\infty} f_y(y)dy \tag{3.27}$$

$$f_x(x) = A_x e^{-a_x x} \sum_{n=0}^{\infty} B_x(n)(x)^n \tag{3.28}$$

$$f_y(y) = A_y e^{-a_y y} \sum_{k=0}^{\infty} B_y(k_1)(y)^k \tag{3.29}$$

$$\int_{z_1}^{\infty} f_x(x)dx = A_x \sum_{n=0}^{\infty} \tilde{B}_x(n)\Gamma(n+1, a_x z_1) \tag{3.30}$$

$$\int_{z_1}^{\infty} f_y(y)dy = A_y \sum_{k=0}^{\infty} \tilde{B}_y(k)\Gamma(k+1, a_y z_1) \tag{3.31}$$

Put the value of $\int_{z_1}^{\infty} f_x(x)dx$ and $\int_{z_1}^{\infty} f_y(y)dy$ in equation (3.27)

$$F(z_1) = 1 - A_x A_y \sum_{k=0}^{\infty}\sum_{n=0}^{\infty} \tilde{B}_x(n)\tilde{B}_y(k)\Gamma(n+1, a_x z_1)\times \Gamma(k+1, a_y z_1) \tag{3.32}$$

Again we simplify the equation (3.32) by using the following formula:

$$\Gamma(t + 1, bq) = e^{-bq} t! \sum_{p=0}^{t} \frac{b^m q^m}{m!} \tag{3.33}$$

$$= 1 - A_x A_y \sum_{k=0}^{\infty} \sum_{n=0}^{\infty} \tilde{B}_x(n) \tilde{B}_y(k) n! e^{-(a_x z_1)} \sum_{i=0}^{n} \frac{a_x^i z_1^i}{i!} \times k! e^{-(a_y z_1)} \sum_{j=0}^{k} \frac{a_y^j z_1^j}{j!} \tag{3.34}$$

$$\overset{(a)}{\cong} 1 - A_x A_y \sum_{k=0}^{\infty} \sum_{n=0}^{\infty} \tilde{B}_x(n) \tilde{B}_y(k) \, n! \, k! \, e^{-(a_x + a_y) z_1} \times \sum_{i=0}^{n} \sum_{j=0}^{k} \frac{a_{x1}^i a_{y1}^j}{i! j!} z_1^{i+j} \tag{3.35}$$

Where $B_x(n) = (K_x^n (1 + K_x)^n / (\omega_x^n(n)^2), B_y(k) = (K_y^k (1 + K_y)^k / (\omega_y^k(k)^2), a_x = (1 + K_x)/\omega_x, a_y = (1 + K_y)/\omega_y, A_x = a_x e^{-K_x}, A_y = a_y e^{-K_y}, \tilde{B}_x(n) = B_x(n)/a_x^{n+1}, \tilde{B}_y(k) = B_y(k)/a_y^{k+1}$.

The subscript x denotes the S-to-D link, y denotes the S-to-R link, w denotes the R-to-D link, and K is the Rician factor. Note that the expansion form of incomplete Gamma function is used for the second equality (a) of (3.35). Then, we prove the convergence of the infinite summation in (3.35) as follows:

- Proof: Let $P_x = (K_x(1 + K_x)/\Omega_x, Q_y = (K_y(1 + K_y)/\Omega_y$, we have

$$\frac{\Gamma(n + 1, a_x z_1)}{n!} < \frac{\Gamma(n + 1)}{n!} < 1 \tag{3.36}$$

$$\frac{\Gamma(k + 1, a_y z_1)}{n!} < \frac{\Gamma(n + 1)}{n!} < 1 \tag{3.37}$$

Then

$$= A_x A_y \sum_{k=0}^{\infty} \sum_{n=0}^{\infty} \tilde{B}_x(n) \tilde{B}_y(k) \Gamma(n + 1, a_x z_1) \times \Gamma(k + 1, a_y z_1) \tag{3.38}$$

$$= A_x A_y \sum_{k=0}^{\infty} \sum_{n=0}^{\infty} \frac{P_x^n}{n!} \frac{Q_y^K}{k!} \frac{\Gamma(n + 1, a_x z_1)}{n!} \frac{\Gamma(k + 1, a_y z_1)}{k!} \tag{3.39}$$

$$< A_x A_y \sum_{k=0}^{\infty} \sum_{n=0}^{\infty} \frac{P_x^n}{n!} \frac{Q_y^K}{k!} \tag{3.40}$$

$$= A_x A_y e^{P_x + Q_y} \tag{3.41}$$

The final value will not change as k or n increases, so the infinite summation in (3.35) is convergent. Similarly, we can obtain the CDF of z_2 as follows:

$$G(z_2) = 1 - \int_{z_2}^{\infty} f_w(w)dw \times \int_{z_2}^{\infty} f_y(y)dy \tag{3.42}$$

$$f_w(w) = A_w e^{-a_w w} \sum_{n=0}^{\infty} B_w(n)(w)^n \tag{3.43}$$

$$f_y(y) = A_y e^{-a_y y} \sum_{k=0}^{\infty} B_y(k)(y)^k \tag{3.44}$$

$$\int_{z_2}^{\infty} f_w(w)dw = A_w \sum_{n=0}^{\infty} \tilde{B}_w(n)\Gamma(n+1, a_w z_2) \tag{3.45}$$

$$\int_{z_2}^{\infty} f_y(y)dy = A_y \sum_{k=0}^{\infty} \tilde{B}_y(k)\Gamma(k+1, a_y z_1) \tag{3.46}$$

Put the value of $\int_{z_2}^{\infty} f_w(w)dw$ and $\int_{z_2}^{\infty} f_y(y)dy$ in equation (3.42)

$$G(z_2) = 1 - A_w A_y \sum_{n=0}^{\infty} \sum_{k=0}^{\infty} \tilde{B}_y(k)\tilde{B}_w(n)\Gamma(n+1, a_w z_2) \times \Gamma(k+1, \frac{a_y}{a_2} z_2) \tag{3.47}$$

$$= 1 - A_w A_y \sum_{k=0}^{\infty} \sum_{n=0}^{\infty} \tilde{B}_w(n)\tilde{B}_{y1}(k_1)n!\, e^{-(a_{w1} z_{22})} \sum_{i=0}^{n} \frac{a_{w1}^i z_{22}^i}{i!} \tag{3.48}$$

$$\times k!\, e^{-(\frac{a_{y1}}{a_2} z_{22})} \sum_{j=0}^{k_1} \frac{(\frac{a_{y1}}{a_2})^j z_2^j}{j!}$$

$$= 1 - A_{w1} A_{y1} \sum_{n_1=0}^{\infty} \sum_{k_1=0}^{\infty} \tilde{B}_{y1}(k_1)\tilde{B}_{w1}(n_1)k_1!\, n_1!\, e^{-(a_{w1}+\frac{a_{y1}}{a_2}) z_{22}} \times \sum_{j=0}^{k_1} \sum_{i=0}^{n_1} \frac{a_{w1}^i (\frac{a_{y1}}{a_2})^j}{i!j!} \tag{3.49}$$

$$z_2^{j+i}$$

where the parameters in (3.49) are similarly defined as those in (3.35).After the CDF of $z_1 \triangleq \min\{\lambda_{SD}, \lambda_{SR}\}$ has been obtained as (3.35),we can substitute it into (3.35), and then the average achievable rate C_{s_1} of the signal s as shown in (3.35) can be expressed as

$$C_{s_1} = \frac{1}{2} \int_0^\infty [\log_2(1 + z_1\rho) - \log_2(1 + z_1\rho a_2)]dF(z_1) \tag{3.50}$$

$$= \frac{1}{2\ln(2)} \left[\rho \int_0^\infty \frac{1 - F(z_1)}{1 + z_1\rho} dz_1 - \rho a_2 \int_0^\infty \frac{1 - F(z_1)}{1 + z_1\rho a_2} dz_1 \right] \tag{3.51}$$

Let $D(\rho) = \rho \int_0^\infty \frac{1-F(z_1)}{1+z_1\rho} dz_1$, and substitute (3.35) into $D(\rho)$, we have

$$D(\rho) = \rho \int_0^\infty \frac{1-F(z_1)}{1+z_1\rho} dz_1 \tag{3.52}$$

$$= A_x A_y \sum_{k=0}^\infty \sum_{n=0}^\infty \widetilde{B}_x(n)\widetilde{B}_y(k)n!\,k! \times \sum_{i=0}^n \sum_{j=0}^k \frac{a_x^i a_y^j}{i!j!} \int_0^\infty \frac{z_1^{i+j}e^{-(a_x+a_y)z_1}}{1+z_1\rho} d(z_1\rho) \tag{3.53}$$

$$\overset{(b)}{=} A_x A_y \sum_{k=0}^\infty \sum_{n=0}^\infty \widetilde{B}_x(n)\widetilde{B}_y(k)n!\,k! \times \sum_{i=0}^n \sum_{j=0}^k \frac{a_x^i a_y^j}{i!j!\rho^{i+j}} \int_0^\infty \frac{t^{i+j}e^{\frac{-(a_x+a_y)z_1}{\rho}}}{1+t} d(t) \tag{3.54}$$

Where (b) is obtained by setting $t = z_1\rho$.

Now we have the following Lemma 1 to calculate the integral $\int_0^\infty \frac{t^{i+j}e^{\frac{-(a_x+a_y)z_1}{\rho}}}{1+t} d(t)$ in (3.54)

Lemma 1: For $m \in \mathbb{Z}^*$ and $\beta > 0$, we have

$$\int_0^\infty \frac{t^m e^{-\beta t}}{1+t} d(t) = e^\beta m!\, \Gamma(-m, \beta) \tag{3.55}$$

Where $\Gamma(-m, \beta) = \int_\beta^\infty \frac{e^{-t}}{t^{m+1}} dt$ denotes the incomplete Gamma function.

Proof: Let $x = \beta(1 + t)$, we have

$$\int_0^\infty \frac{t^m e^{-\beta t}}{1+t} d(t) = \frac{e^\beta}{\beta^m} \int_\beta^\infty \frac{(x-\beta)^m e^{-x}}{x} dx \tag{3.56}$$

Then we define :

$$J_m(x) = \frac{(x-\beta)^m}{x}, \tag{3.57}$$

$$I(x) = \frac{e^\beta}{\beta^m} \int_\beta^\infty J_m(x)\, e^{-x} dx \tag{3.58}$$

On the one hand, by substituting (3.57) into (3.58), we have

$$I(x) = -\frac{e^\beta}{\beta^m} \int_\beta^\infty \frac{(x-\beta)^m e^{-x}}{x} d(e^{-x}) \tag{3.59}$$

$$= -\frac{e^\beta}{\beta^m} \left.\frac{(x-\beta)^m e^{-x}}{x}\right|_\beta^\infty + \frac{e^\beta}{\beta^m} \int_\beta^\infty \frac{(x-\beta)^{m-1}(mx-x-\beta)}{x^2} e^{-x} d(x) \tag{3.60}$$

$$= \frac{e^\beta}{\beta^m} \int_\beta^\infty J_{m-1}(x)\, e^{-x} dx \tag{3.61}$$

We can observe from (3.61) that as long as β is a root of $J_m(x)$),the integral can be successively calculated by using (3.61) for m times.On the other hand, we know that $J_m(x) = \frac{(x-\beta)^m}{x} = x^{m-1}$ $+a_{m-2}x^{m-2} + ... + a_0 + (-1)^m \beta^m /x$, so after m times of integration by part, we will have

$$\tag{3.62}$$

$$I(x) = -\frac{e^\beta}{\beta^m} \int_\beta^\infty \frac{(x-\beta)^m e^{-x}}{x} d(e^{-x}) \tag{3.62}$$

$$I(x) = -\frac{e^\beta}{\beta^m} \int_\beta^\infty \left(x^{m-1} + ... + a_0 + (-1)^m \frac{\beta^m}{x}\right)^{(m)} d(e^{-x}) \tag{3.63}$$

$$I(x) = -\frac{e^\beta}{\beta^m} \int_\beta^\infty \left((-1)^m \frac{\beta^m}{x}\right)^{(m)} d(e^{-x}) \tag{3.64}$$

$$= e^\beta m!\, \Gamma(-m, \beta) \tag{3.65}$$

where $(\cdot)^{(m)}$ denotes m-order derivation. Substitute (3.55) in Lemma 1 into (3.54), we can get the final exact expression of C_{s_1} as

$$C_{s_1} = \frac{1}{2ln(2)}(D(\rho) - D(\rho a_2)) \tag{3.67}$$

Where

$$D(\rho) = A_x A_y \sum_{k=0}^{\infty} \sum_{n=0}^{\infty} \tilde{B}_x(n)\tilde{B}_y(k)n!\,k! \times \sum_{i=0}^{n} \sum_{j=0}^{k} \frac{(i+j)!a_x^i a_y^j}{i!j!\rho^{i+j}} e^{\frac{-(a_x+a_y)}{\rho}} \Gamma\left(-i - j, \frac{(a_x+a_y)}{\rho}\right) \tag{3.68}$$

and $D(\rho a_2)$ shares the same form as $D(\rho)$. Similarly, we can derive the exact expression of C_{s_2} as

$$C_{s_2} = \frac{1}{2ln(2)}A_x A_y \sum_{k=0}^{\infty} \sum_{n=0}^{\infty} \tilde{B}_x(n)\tilde{B}_y(k)n!\,k! \times \sum_{i=0}^{n} \sum_{j=0}^{k} \frac{(i+j)!a_w^i (\frac{a_y}{a_2})^j}{i!j!\rho^{i+j}} e^{\frac{-\left(a_w+\frac{a_y}{a_2}\right)}{\rho}} \Gamma\left(-i - j, \frac{\left(a_w+\frac{a_y}{a_2}\right)}{\rho}\right), \tag{3.69}$$

Although we have derived the exact expressions of the achievable rates of s1 and s2 in (3.67) and (3.69) respectively, such expressions are very complicated, since the incomplete Gamma function is difficult to calculate. Thus, it is still difficult to get the exact values of the achievable rates, which motivates us to propose an approximation method to solve this problem in the next subsection.

3.3 Achievable Rate Approximation:

In this subsection, we propose an approximation method using Gauss-Chebyshev Integration [12] to simplify the numerical calculation of the incomplete Gamma function $\Gamma(-m,\beta)$. However,

Gauss-Chebyshev Integration is used on the limited interval $[-1, 1]$, while the integral intervals incomplete Gamma functions of (3.67) and (3.69) are infinite intervals. Thus,we set $t = 2\beta\frac{1}{x} - 1$ and convert the incomplete Gamma function as

$$\Gamma(-m, \beta) = \left(\frac{1}{2\beta}\right)^m \int_{-1}^{1} \frac{1}{\sqrt{1-t^2}} (t+1)^{m-1} e^{\frac{-2\beta}{t+1}} \sqrt{1-t^2} \, dt \tag{3.70}$$

$$= \left(\frac{1}{2\beta}\right)^m \frac{\pi}{n} \sum_{i=1}^{n} \left(\cos\left(\frac{2l-1}{2n}\pi\right) + 1\right)^{m-1} \times e^{-\frac{2\beta}{\cos\left(\frac{2l-1}{2n}\pi\right)+1}} \left|\sin\left(\frac{2l-1}{2n}\pi\right)\right| \tag{3.80}$$

where n is the approximation order. Substituting (3.26) into the exact expression of the achievable rate (3.23), we can finally obtain the approximation of (3.23) as

$$C_{s_1} = \frac{1}{2ln(2)} (D(\rho) - D(\rho a_2)), \tag{3.81}$$

where

$$D(\rho) = \tag{3.82}$$

$$A_x A_y \sum_{k=0}^{\infty} \sum_{n=0}^{\infty} \tilde{B}_x(n)\tilde{B}_y(k)n! \, k! \times$$

$$\sum_{i=0}^{n} \sum_{j=0}^{k} \frac{(i+j)! a_x^i a_y^j}{i! j! \rho^{i+j}} \times e^{\frac{-(a_x+a_y)}{\rho}} \left(\frac{1}{2\frac{(a_x+a_y)}{\rho}}\right)^{i+j} \frac{\pi}{n} \sum_{l=1}^{n} \left(\cos\left(\frac{2l-1}{2n}\pi\right) + 1\right)^{i+j-1} \times$$

$$e^{-\frac{2\frac{(a_x+a_y)}{\rho}}{\cos\left(\frac{2l-1}{2n}\pi\right)+1}} \left|\sin\left(\frac{2l-1}{2n}\pi\right)\right|$$

and $D(\rho a_2)$ shares the same form as $D(\rho)$. Similarly, (3.69) can be approximated as

$$C_{s_2} = \tag{3.83}$$

$$\frac{1}{2ln(2)} A_x A_y \sum_{k=0}^{\infty} \sum_{n=0}^{\infty} \tilde{B}_x(n)\tilde{B}_y(k)n! \, k! \times$$

$$\sum_{i=0}^{n} \sum_{j=0}^{k} \frac{(i+j)! a_w^i (\frac{a_y}{a_2})^j}{i! j! \rho^{i+j}} \times e^{\frac{\left(a_x+\frac{a_y}{a_2}\right)}{\rho}} \left(\frac{1}{2\frac{\left(a_w+\frac{a_y}{a_2}\right)}{\rho}}\right)^{i+j} \frac{\pi}{n} \sum_{l=1}^{n} \left(\cos\left(\frac{2l-1}{2n}\pi\right) + 1\right)^{i+j-1} \times$$

$$e^{-\frac{2\frac{\left(a_w+\frac{a_y}{a_2}\right)}{\rho}}{\cos\left(\frac{2l-1}{2n}\pi\right)+1}} \left|\sin\left(\frac{2l-1}{2n}\pi\right)\right|,$$

Thus, the approximated achievable rates (3.81) and (3.83) can be conveniently calculated numerically, and their accuracy will be validated by the simulation results in the next chapter.

CHAPTER-4

RESULT

In this chapter, we compare the analytical results obtained in the previous chapter with Monte Carlo simulations to validate their accuracy. Specifically, 10^5 realizations of Rician distribution random variables are generated, and the approximation order for Gauss-Chebyshev Integration is set as 100.
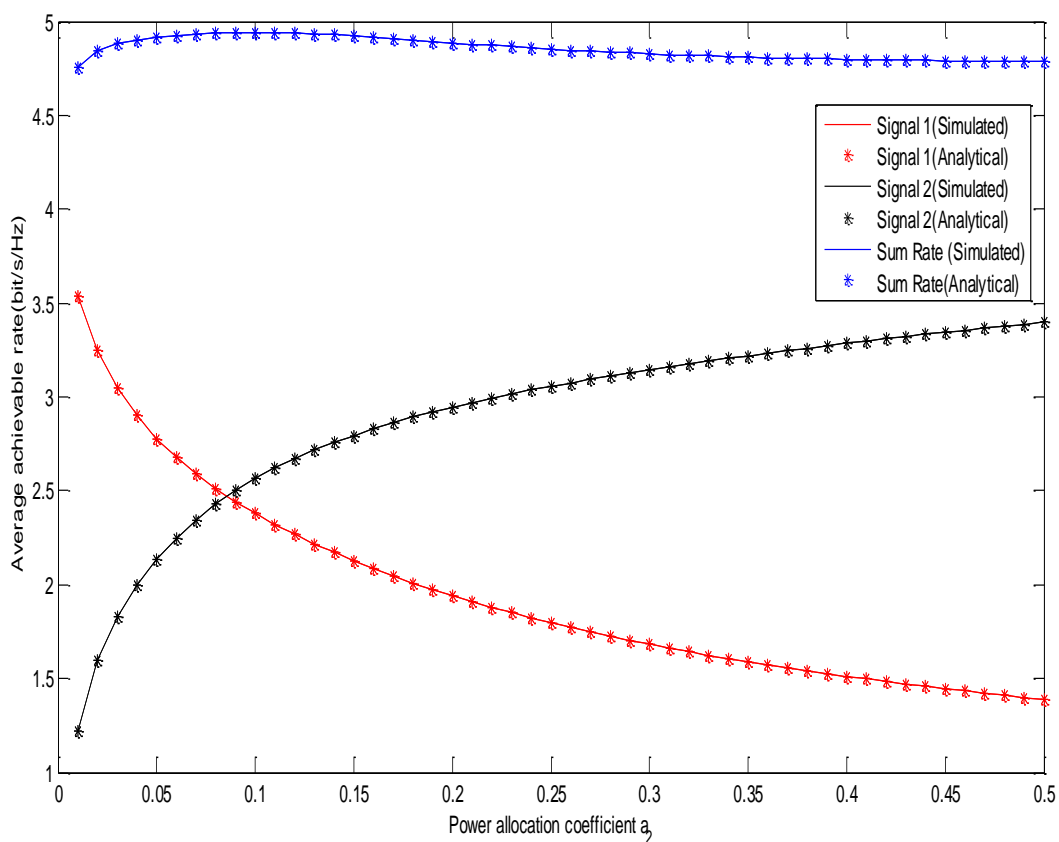

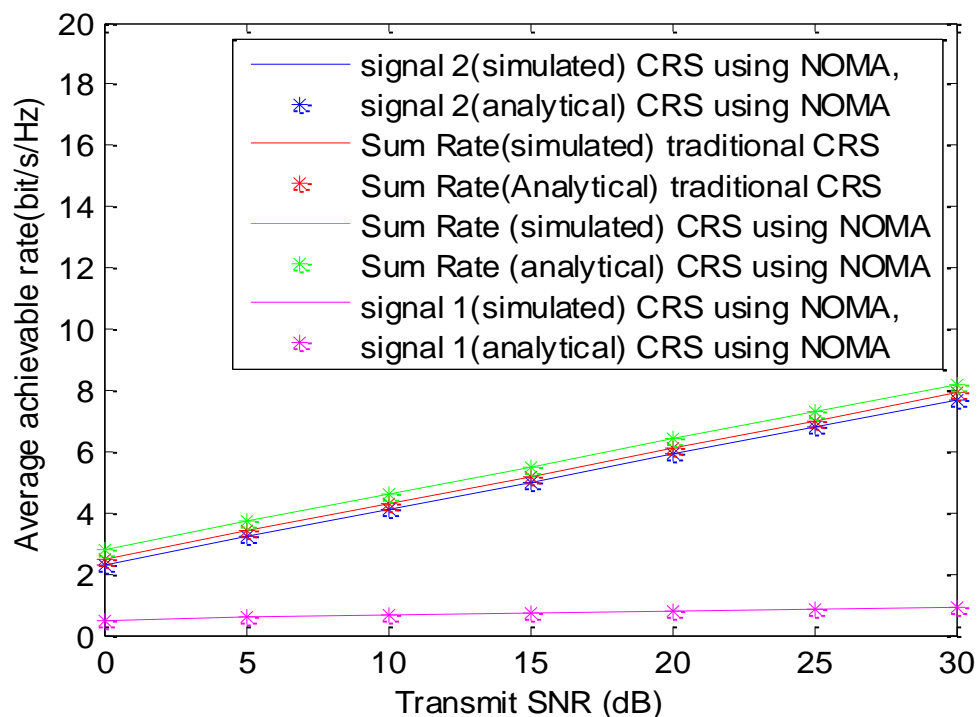**Figure 4.1.** Achievable rates for the NOMA-based CRS over Rician fading channels.

Figure. 4.2. Achievable rates comparison between the NOMA based CRS and traditional CRS.

Fig. 4.1 presents the achievable rate performance of s1, s2 and the corresponding sum rate of the NOMA-based CRS against the power allocation coefficient a_2. In the model of Rician fading channel, the parameter Ω denotes the average power gain of the channel [13], which is usually determined by distances between transceivers. In our system , Ω_i ($i \in \{SD, SR, RD\}$) denotes the average power gain of link SD, link SR, and link RD, mainly reflecting the impacts of distances from S to D, from S to R, and from R to D, respectively. Thus, we set $\Omega_{SD} = 9 < \Omega_{SR} = \Omega_{RD} = 36$ [10], because the distances from S to R and from R to D are usually smaller than the distance from S to D, and thus link SR and link RD have higher average power gains than link SD. According to [11], other parameters are set as SNR = 20 dB, $K_{SR} = K_{RD} = 5$, and $K_{SD} = 2$. From Fig. 4.1, we can observe that the derived analytical results using Gauss-Chebyshev Integration match well with the simulation results. In addition, as a_2 increases, s2 will get more power and its achievable rate increases accordingly, while the achievable rate of s1 decreases. Moreover, the sum rate of two signals first increases and then slowly decreases with the increase of a_2. Actually, we can see from (3.22) that when a_2 is small, the achievable rate of s_2 is mainly

determined by link SR, as $a_2\lambda_{SR}$ will always be smaller than λ_{RD} . Due to SIC, s_2 will have no interference in link SR, so increasing a_2 will largely increase the achievable rate of s_2, and thus increase the sum rate. However, when a_2 increases, $a_2\lambda_{SR}$ will be larger than λ_{RD} at last, and the rate of link RD will slowly become the determinant factor, which is not influenced by a_2.As a result, the increase of s_2 achievable rate finally cannot make up for the decrease of s_1's achievable rate, which causes the decrease of the sum rate, as shown in Fig. 4.1. Thus, there exists an optimal power allocation coefficient to maximize the sum rate, which is an interesting research topic deserving further investigation in the future. Fig. 4.2 compares the achievable rates of the traditional CRS and the NOMA-based CRS against the transmit SNR, where we set $a_2 = 0.4, \Omega_{SD} = 9$, $\Omega_{RD} = 36$, and $\Omega_{SR} = 144$. We find that the simulation results and analytical results are consistent, and the NOMA-based CRS achieves higher achievable sum rate than the traditional CRS, since NOMA-based CRS can transmit two signals in two slots, while traditional CRS can only transmit one signal during the same time.

CONCLUSION

In this thesis, we have investigated the performance of a NOMA based cooperative relaying system by deriving the exact analytical expressions of the achievable rates. Moreover, an efficient approximation method using Gauss-Chebyshev Integration for the achievable rates was also proposed, which enables the sum series of the achievable rate expressions converge quickly. Simulation results have verified that our derived analytical results match well with the Monte Carlo simulations, and the NOMA-based CRS is able to achieve higher achievable rate than the traditional CRS.

REFERENCES

[1] K. J. R. Liu, A. K. Sadek,W. Su, and A. Kwasinski, Cooperative Communications and Networking. New York City, NY, USA: Cambridge University Press, 2009.

[2] P. N. Son and H. Y. Kong, "Cooperative communication with energy-harvesting relays under physical layer security," IET Commun., vol. 9, no. 17, pp. 2131–2139, Nov. 2015.

[3] R. Fan, J. Cui, S. Jin, K. Yang, and J. An, "Optimal node placement and resource allocation for UAV relaying network," IEEE Commun. Lett., vol. 22, no. 4, pp. 808–811, Apr. 2018.

[4] M. Ju and H.-C. Yang, "Optimum design of energy harvesting relay for two-way decode-and forward relay networks under max-min and max-sum criterions," IEEE Trans. Commun., vol. 67, no. 10, pp. 6682–6697, Oct. 2019.

[5] K. Sultan, "Best relay selection schemes for NOMA based cognitive relay networks in underlay spectrum sharing," IEEE Access, vol. 8, pp. 190 160–190 172, 2020.

[6] A. Sendonaris, E. Erkip, and B. Aazhang, "User cooperation diversity-part I: System description,"IEEE Trans. Commun., vol. 51, no. 11, pp. 1927–1938, Nov. 2003.

[7] ——, "User cooperation diversity-part II: Implementation aspects and performance analysis," IEEE Trans. Commun., vol. 51, no. 11, pp. 1939–1948, Nov. 2003.

[8] R. U. Nabar, H. Bolcskei, and F. W. Kneubuhler, "Fading relay channels: Performance limits and space-time signal design," IEEE J. Sel. Areas Commun., vol. 22, no. 6, pp. 1099–1109, Aug. 2004.

[9] H. Cui, L. Song, and B. Jiao, "Multi-pair two-way amplify-and-forward relaying with very large number of relay antennas," IEEE Trans. Wireless Commun., vol. 13, no. 5, pp. 2636–2645, May 2014.

[10] S. Luo and K. C. Teh, "Amplify-and-forward based two-way relay arq system with relay combination,"IEEE Commun. Lett., vol. 19, no. 2, pp. 299–302, Feb. 2015.

[11] D. Li, "Amplify-and-forward relay sharing for both primary and cognitive users," IEEE Trans. Veh.Technol., vol. 65, no. 4, pp. 2796–2801, Apr. 2016.

[12] Y. Dong, M. J. Hossain, and J. Cheng, "Performance of wireless powered amplify and forward relaying over Nakagami-mfading channels with nonlinear energy harvester," IEEE Commun. Lett.,vol. 20, no. 4, pp. 672–675, Apr. 2016.

[13] S. Li, K. Yang, M. Zhou, J. Wu, L. Song, Y. Li, and H. Li, "Full-duplex amplify-and-forward relaying: Power and location optimization," IEEE Trans. Veh. Technol., vol. 66, no. 9, pp. 8458– 8468, Sep. 2017.

[14] K. M. Rabie and B. Adebisi, "Enhanced amplify-and-forward relaying in non-Gaussian PLC networks,"IEEE Access, vol. 5, pp. 4087–4094, 2017.

[15] L. Jiang and H. Jafarkhani, "mmWave amplify-and-forward MIMO relay networks with hybrid precoding/combining design," IEEE Trans. Wireless Commun., vol. 19, no. 2, pp. 1333–1346, Feb. 2020.

[16] A. S. Ibrahim, A. K. Sadek, W. Su, and K. J. R. Liu, "Cooperative communications with relay selection:When to cooperate and whom to cooperate with?" IEEE Trans. Wireless Commun., vol. 7, no. 7, pp. 2814–2827, Jul. 2008.

[17] M. R. Bhatnagar, R. K. Mallik, and O. Tirkkonen, "Performance evalution of best-path selection in a multihop decode-and-forward cooperative system," IEEE Trans. Veh. Technol., vol. 65, no. 4, pp.2722–2728, Apr. 2016.

[18] Y. Gu and S. Aissa, "RF-based energy harvesting in decode-and-forward relaying systems: Ergodic and outage capacities," IEEE Trans. Wireless Commun., vol. 14, no. 11, pp. 6425–6434, Nov. 2015.

[19] G. T. Djordjevic, K. Kansanen, and A. M. Cvetkovic, "Outage performance of decode-and-forward cooperative networks over Nakagami-m fading with node blockage," IEEE Trans. Wireless Commun.,vol. 15, no. 9, pp. 5848–5860, Sep. 2016.

[20] H. Liu, Z. Ding, K. J. Kim, K. S. Kwak, and H. V. Poor, "Decode-and-forward relaying for cooperative NOMA systems with direct links," IEEE Trans. Wireless Commun., vol. 17, no. 12, pp.8077–8093, Dec. 2018.

[21] R. Fan, S. Atapattu, W. Chen, Y. Zhang, and J. Evans, "Throughput maximization for multihop decode-and-forward relay network with wireless energy harvesting," IEEE Access, vol. 6, pp.24 582–24 595, 2018.

[22] O. M. Kandelusy and S. M. H. Andargoli, "Outage performance of decode-and-forward (DF)-based multiuser spectrum sharing relay system with direct link in the presence of primary users' power,"IET Commun., vol. 12, no. 3, pp. 246–254, Feb. 2018.

[23] E. Li, X. Wang, Z. Wu, S. Hao, and Y. Dong, "Outage analysis of decode-and-forward two-way relay selection with different coding and decoding schemes," IEEE Syst. J., vol. 13, no. 1, pp.125–136, Mar. 2019.

[24] M. Asadpour, B. Van den Bergh, D. Giustiniano, K. A. Hummel, S. Pollin, and B. Plattner, "Micro aerial vehicle networks: an experimental analysis of challenges and opportunities," IEEE Commun.Mag., vol. 52, no. 7, pp. 141–149, Jul. 2014.

[25] K. Namuduri, S. Chaumette, J. H. Kim, and J. P. G. Sterbenz, UAV Networks and Communications. Cambridge University Press, 2017.

[26] K. P. Valavanis and G. J. Vachtsevanos, Handbook of Unmanned Aerial Vehicles. Springer, 2015.

[27] F. Ono, H. Ochiai, and R. Miura, "A wireless relay network based on unmanned aircraft system with rate optimization," IEEE Trans. Wireless Commun., vol. 15, no. 11, pp. 7699–7708, Nov. 2016.

[28] M. M. Azari, F. Rosas, K.-C. Chen, and S. Pollin, "Ultra reliable UAV communication using altitude and cooperation diversity," IEEE Trans. Commun., vol. 66, no. 1, pp. 330–344, Jan. 2018.

[29] M. M. Azari, F. Rosas, and P. Sofie, "Cellular connectivity for UAVs: Network modeling, performance analysis, and design guidelines," IEEE Trans. Wireless Commun., vol. 18, no. 7, pp.3366–3381, Jul. 2019.

[30] W. Wang, X. Li, M. Zhang, K. Cumannan, D. W. K. Ng, G. Zhang, J. Tang, and O. A. Dober, "Energy-constrained UAV-assisted secure communications with position optimization and cooperative jamming," IEEE Trans. Commun., vol. 68, no. 7, pp. 4476–4489, Jul. 2020.

[31] H. Shakhatreh, A. H. Sawalmeh, A. Al-Fuqaha, Z. Dou, E. Almaita, I. Khalil, N. S. Othman, A. Khreishah, and M. Guizani, "Unmanned aerial vehicles (UAVs): A survey on civil applications and key research challenges," IEEE Access, vol. 7, pp. 48 572–48 634, 2019.

[32] W. Ejaz, M. A. Azam, S. Saadat, F. Iqbal, and A. Hanan, "Unmanned aerial vehicle enabled IoT platform for disaster management," Energies, vol. 12, no. 14, p. 2706, Jul. 2019.

[33] Y. Zeng, R. Zhang, and T. J. Lim, "Wireless communications with unmanned aerial vehicles: opportunities and challenges," IEEE Commun. Mag., vol. 54, no. 5, pp. 36–42, May 2016.

[34] J. Zhao, F. Gao, Q. Wu, S. Jin, Y. Wu, and W. Jia, "Beam tracking for UAV mounted Sat Com on the-move with massive antenna array," IEEE J. Sel. Areas Commun., vol. 36, no. 2, pp. 363–375,Feb. 2018.

[35] Y. Zeng, R. Zhang, and T. J. Lim, "Throughput maximization for UAV-enabled mobile relaying systems," IEEE Trans. Commun., vol. 64, no. 12, pp. 4983–4996, Dec. 2016.

[36] Y. Zhang, Z. Mou, F. Gao, L. Xing, J. Jiang, and Z. Han, "Hierarchical deep reinforcement learning for backscattering data collection with multiple UAVs," IEEE Internet Things J., vol. 8, no. 5, pp.3786–3800, Mar. 2021.

[37] J. Zhao, Y. Wang, Z. Fei, X. Wang, and Z. Miao, "NOMA-aided UAV data collection system: Trajectory optimization and communication design," IEEE Access, vol. 8, pp. 155 843–155 858,2020.

[38] F. Luo, C. Jiang, J. Du, J. Yuan, Y. Ren, S. Yu, and M. Guizani, "A distributed gateway selection algorithm for UAV networks," IEEE Trans. Emerg. Topics Comput., vol. 3, no. 1, Mar. 2015.

[39] R. Duan, J. Wang, C. Jiang, Y. Ren, and L. Hanzo, "The transmit-energy vs computation-delay trade-off in gateway-selection for heterogenous cloud aided multi-UAV systems," IEEE Trans.Commun., vol. 67, no. 4, pp. 3026–3039, Apr. 2019.

[40] M. Vaezi, R. Schober, Z. Ding, and H. V. Poor, "Non-orthogonal multiple access: Common myths and critical questions," IEEE Wireless Commun., vol. 26, no. 5, pp. 174–180, Oct. 2019.

[41] M. Vaezi and H. V. Poor, "NOMA: An information-theoretic perspective," in Multiple Access Techniques for 5G Wireless Networks and Beyond, M. Vaezi, Z. Ding, and H. V. Poor, Eds. Cham:Springer International Publishing, 2019, pp. 167–193.

[42] F. Mokhtari, M. R. Milli, F. Eslami, F. Ashtiani, B. Makki, M. Mirmohseni, M. Nasiri-Kenari, and T. Svensson, "Download elastic traffic rate optimization via NOMA protocols," IEEE Trans. Veh. Technol., vol. 68, no. 1, pp. 713–727, Jan. 2019.

[43] Z. Ding, M. Peng, and H. V. Poor, "Cooperative non-orthogonal multiple access in 5G systems,"IEEE Commun. Lett., vol. 19, no. 8, pp. 1462–1465, Aug. 2015.

[44] S. M. R. Islam, N. Avazov, O. A. Dobre, and K.-s. Kwak, "Power-domain non-orthogonal multiple access (NOMA) in 5G systems: Potentials and challenges," IEEE Commun. Surveys Tuts., vol. 19, no. 2, pp. 721–742, Second quarter 2017.

[45] 3GPP, "Study on network-assisted interference cancellation and suppression (NAICS) for LTE v.12.0.1," 3rd Generation Partnership Project (3GPP), Sophia Antipolis, France, Rep. TR 36.866, Mar. 2014.

[46] Media Tek, "Study on downlink multiuser superposition transmission (MUST) for LTE," 3rd Generation Partnership Project (3GPP), Hsinchu, Taiwan, Rep. TR 36.859, Apr. 2015.

[47] B. Wu, J. Chen, J. Wu, and M. Cardei, "A survey of attacks and countermeasures in mobile ad hoc networks," in Wireless Network Security, Y. Xiao, X. S. Shen, and D.-Z. Du, Eds. Boston, MA,USA: Springer, 2007, ch. 5, pp. 103–135.

[48] Y. Wang, G. Attebury, and B. Ramamurthy, "A survey of security issues in wireless sensor networks,"IEEE Commun. Surveys Tuts., vol. 8, no. 2, pp. 2–23, Second Quarter 2006.

[49] T. T. Karygiannis and L. Owens, "Wireless network security: 802.11, bluetooth and handheld devices," Gaithersburg, MD, USA, Nov. 2002.

[50] P. W. Shor, "Algorithms for quantum computation: discrete logarithms and factoring," in Proc.IEEE Annu. Symp. Found. of Comput. Sci. (FOCS), Santa Fe, NM, USA, Nov. 1994.

[51] R. K. Nichols and P. C. Lekkas, Wireless Security: Models, Threats, and Solutions. New York,NY, USA: McGraw-Hill, 2002.

[52] M. Bloch and J. Barros, Physical-Layer Security: From Information Theory to Security Engineering.Cambridge, United Kingdom: Cambridge University Press, 2011.

[53] A. D. Wyner, "The wire-tap channel," Bell Syst. Tech. J., vol. 54, no. 8, pp. 1355–1387, 1975.

[54] I. Csiszar and J. Korner, "Broadcast channels with confidential messages," IEEE Trans. Inf. Theory,vol. 24, no. 3, pp. 339–348, May 1978.

[55] S. Leung-Yan-Cheong and M. Hellman, "The Gaussian wire-tap channel," IEEE Trans. Inf. Theory,vol. 24, no. 4, pp. 451–456, Jul. 1978.

[56] E. Tekin and A. Yener, "The general Gaussian multiple-access and two-way wiretap channels:Achievable rates and cooperative jamming," IEEE Trans. Inf. Theory, vol. 54, no. 6, pp. 2735–2751, Jun. 2008.

[57] J. Huang and A. L. Swindlehurst, "Cooperative jamming for secure communications in MIMO relay networks," IEEE Trans. Signal Process., vol. 59, no. 10, pp. 4871–4884, Oct. 2011.

[58] X. He and A. Yener, "Providing secrecy with structured codes: Two-user Gaussian channels," IEEE Trans. Inf. Theory, vol. 60, no. 4, pp. 2121–2138, Apr. 2014.

[59] P. Mukherjee, J. Xie, and S. Ulukus, "Secure degree of freedom of one-hop wireless networks with no eavesdropper CSIT," IEEE Trans. Inf. Theory, vol. 63, no. 3, pp. 1898–1922, Mar. 2017.

[60] I. Krikidis, J. S. Thompson, and S. Mclaughlin, "Relay selection for secure cooperative network, "IEEE Trans. Wireless Commun., vol. 8, no. 10, pp. 5003–5011, Oct. 2009.

[61] R. Bassily and S. Ulukus, "Deaf cooperation and relay selection strategies for secure communication in multiple relay networks," IEEE Trans. Signal Process., vol. 61, no. 6, pp. 1544–1554, Mar.2013.

[62] G. Chen, Z. Tian, Y. Gong, Z. Chen, and J. A. Chambers, "Max-ratio relay selection in secure buffer-aided cooperative wireless networks," IEEE Trans. Inf. Forensics Security, vol. 9, no. 4, pp.719–729, Apr. 2014.

[63] X. Liao, Y. Zhang, Z. Wu, Y. Shen, X. Jiang, and H. Inamura, "On security-delay trade-off in two hop wireless networks with buffer-aided relay selection," IEEE Trans. Wireless Commun., vol. 17,no. 3, pp. 1893–1906, Mar. 2018.

[64] A. Khisti and G.W.Wornell, "Secure transmission with multiple antennas I: The MISOME wiretap channel," IEEE Trans. Inf. Theory, vol. 56, no. 7, pp. 3088–3104, Jul. 2010.

[65] ——, "Secure transmission with multiple antennas – Part II: The MIMOME wiretap channel,"IEEE Trans. Inf. Theory, vol. 56, no. 11, pp. 5515–5532, Nov. 2010.

[66] R. Feng, M. Dai, and H. Wang, "Distributed beamforming in MISO SWIPT system," IEEE Trans.Veh. Technol., vol. 66, no. 6, pp. 5440–5445, Jun. 2017.

[67] F. Zhu, F. Gao, M. Yao, and H. Zou, "Joint information- and jamming-beamforming for physical layer security with full duplex base station," IEEE Trans. Signal Process., vol. 62, no. 24, pp.6391–6401, Dec. 2014.

[68] B. Medepally and N. B. Mehta, "Voluntary energy harvesting relays and selection in cooperative wireless networks," IEEE Trans. Wireless Commun., vol. 9, no. 11, pp. 3543–3553, Nov. 2010.

[69] H. Al-Tous and I. Barhumi, "Reinforcement learning framework for delay sensitive energy harvesting wireless sensor networks," IEEE Sensors J., vol. 21, no. 5, pp. 7103–7113, Mar. 2021.

[70] K. W. Choi, A. A. Aziz, D. Setiawan, N. M. Tran, L. Ginting, and D. I. Kim, "Distributed wireless power transfer system for Internet of Things devices," IEEE Internet Things J., vol. 5, no. 4, pp.2657–2671, Aug. 2018.

[71] A. Goldsmith, Wireless Communications. Cambridge, United Kingdom: Cambridge university press, 2005.

[72] F. Boccardi, R. W. Heath, A. Lozano, T. L. Marzetta, and P. Popovski,"Five disruptive technology directions for 5G," IEEE Commun. Mag.,vol. 52, no. 2, pp. 74–80, Feb. 2014.

[73] L. Dai, B. Wang, Y. Yuan, S. Han, C.-L. I, and Z. Wang, "Non orthogonal multiple access for 5G: Solutions, challenges, opportunities, and future research trends," IEEE Commun. Mag., vol. 53, no. 9,pp. 74–81, Sep. 2015.

[74] F. Fang, H. Zhang, J. Cheng, and V. Leung, "Energy-efficient resource allocation for downlink non-orthogonal multiple access network," IEEE Trans. Commun., vol. 64, no. 9, pp. 3722–3732, Sep. 2016.

[75] Y. Sun, D. Ng, Z. Ding, and R. Schober, "Optimal joint power and subcarrier allocation for full-duplex multicarrier non-orthogonal multiple access systems," IEEE Trans. Commun., vol. 65, no. 3,pp. 1077–1091, Mar. 2017.

[76] Y. Saito, A. Benjebbour, Y. Kishiyama, and T. Nakamura, "System level performance evaluation of downlink non-orthogonal multiple access (NOMA)," in Proc. IEEE Annu. Symp. Pers. Indoor Mobile Radio Commun., London, U.K., Sep. 2013, pp. 611–615.

[77] L. Liu, C. Yuen, Y. L. Guan, and Y. Li, "Capacity-achieving iterative LMMSE detection for MIMO-NOMA systems," in Proc. IEEE Int. Conf.Commun., Kuala Lumpur, Malaysia, May 2016, pp. 1–6.

[78] J. N. Laneman, D. N. Tse, and G. W. Wornell, "Cooperative diversity in wireless networks: Efficient protocols and outage behavior," IEEE Trans.Inf. Theory, vol. 50, no. 12, pp. 3062–3080, Dec. 2004.

[79] Y. Liu, Z. Ding, M. Elkashlan, and H. V. Poor, "Cooperative non orthogonal multiple access with simultaneous wireless information and power transfer," IEEE J. Sel. Areas Commun., vol. 34, no. 4, pp. 938–953,Apr. 2016.

[80] Z. Ding, M. Peng, and H. V. Poor, "Cooperative non-orthogonal multiple access in 5G systems," IEEE Commun. Lett., vol. 19, no. 8, pp. 1462–1465,Aug. 2015.

[81] J.-B. Kim and I.-H. Lee, "Capacity analysis of cooperative relaying systems using non-orthogonalmultiple access," IEEE Commun. Lett., vol. 19,no. 11, pp. 1949–1952, Nov. 2015.

[82] M. R. Bhatnagar, "On the capacity of decode-and-forward relaying over Rician fading channels," IEEE Commun. Lett., vol. 17, no. 6, pp. 1100–1103, Jun. 2013.

[83] E. Hildebrand, Introduction to Numerical Analysis. New York, NY, USA:Dover, 1987.

[84] A. Abdi, C. Tepedelenlioglu, M. Kaveh, and G. Giannakis, "On the estimation of the K parameter for the rice fading distribution," IEEE Commun. Lett., vol. 5, no. 3, pp. 92–94, Mar. 2001.

Performance Analysis of Cooperative NOMA System

Sabra Akhtar Siddiqui[1], Saif Ahmad[2], Mohd Javed Khan[3]
[1, 2, 3] Dept of ECE
[1, 2, 3] Integral University, Lucknow, U.P.

Abstract- *A technology that holds promises for fifth generation (5G) wireless communications is non-orthogonal multiple access (NOMA). The integration of NOMA with cooperative relaying has lately gained growing interest because users with good channel conditions can function as relays to improve the system performance by using successive interference cancellation (SIC).*

An analytical approach for assessing the performance of a cooperative relaying system based on NOMA is proposed in this research. The exact expression of the average achievable rate is derived after studying NOMA's performance over Rician fading channels. In addition, we also suggest a Gauss-Chebyshev integration-based approximation method to determine the feasible rate. The numerical results support the strong match between our derived analytical results and the Monte Carlo simulations.

Keywords- NOMA, 5G, SIC, Rician fading, cooperative relaying.

I. INTRODUCTION

It is highly expected that future 5G networks should achieve a 10-fold increase in connection density, i.e., 106 connections per square kilometers [1]. Non-orthogonal multiple access (NOMA) has been proposed as a promising candidate to realize such an aggressive 5G goal [2]–[5]. NOMA is fundamentally different from conventional orthogonal multiple access (OMA) schemes such as FDMA, TDMA, OFDMA, etc., since it allows multiple users to simultaneously transmit signals using the same time/frequency radio resources but different power levels [3]–[5]. The key advantage of NOMA is to explore the extra power domain to further increase the number of supportable users. Specifically, users are identified by their channel conditions, those with good channel conditions are called strong users and others are called weak users. For the sake of fairness, less power are allocated to strong users at the transmitter side. In this way, the transmitter sends the superposition of signals with different power levels and the receiver applies successive interference cancellation (SIC) to strong users to realize multi-user detection [5], [6]. Such non-orthogonal resource allocation enables NOMA to accommodate more users and makes it promising to address the 5G requirement of massive

connectivity, with the cost of controllable increase of complexity in receiver design due to SIC [5].In NOMA systems, the use of SIC implies that strong users have prior information about the messages of other users, so essentially they are able to serve as cooperative relays. Moreover, cooperative relaying is able to significantly enhance the system performance of cellular networks [7]. Thus, combining cooperative relaying and NOMA is promising to improve the throughput of future 5G wireless networks, and has attracted increasing interests recently [8]. Specifically, a cooperative NOMA transmission scheme was proposed in [9], where strong users decode the signals that are intended to others and serve as relays to improve the performance of weak users. Another NOMA-based cooperative scheme was proposed in [10], where the performance of a NOMA-based decode-and-forward relaying system under Rayleigh fading channel was studied. However, most of existing NOMA schemes only consider the Rayleigh fading channel, which is suitable for rich scattering scenarios without line of sight (LOS), while little attention has been drawn to the more general Rician fading channel, which takes both LOS and non LOS (NLOS) into consideration. In some typical 5G application scenarios, such as massive machine-type communications (mMTC) and Internet of things (IoT), "users" may be low-cost sensors deployed in a small area, where both LOS and NLOS exist, which can be better modeled by the Rician fading channel. In this paper, we investigate the performance of the NOMA-based cooperative relaying transmission scheme in [10] under Rician fading channels1 Evaluating system performance under Rician fading channel is rather challenging as the probability density function of Rician distribution variables consists of Bessel function, which makes it difficult to calculate the average achievable rate through integration. In order to derive the exact expression of the achievable rate, we propose an analytical method using Taylor expansion of Bessel function and incomplete Gamma function. However, the complexity of the incomplete Gamma function makes it still difficult to get the exact values, so we further propose an approximation method using Gauss-Chebyshev Integration to simplify the calculation. Finally, simulations confirm that our analytical results match well with the Monte Carlo results.

Comparing with wired communication, the wireless network has been the practical communication method due to its convenience and flexibility in varies environments. In

conjunction with the development of the beyond fifth-generation (5G) and sixth-generation (6G) mobile communications, various kinds of Internet of Things (IoT) devices (e.g., smart phones, smart watches and other IoT sensors) are designed and produced. The number of these devices is predicted to keep increasing in the upcoming years. Therefore, connecting massive number of devices through wireless signals will become more important. The most critical challenge for wireless systems is to find practical solutions in performance and secrecy improvement, i.e., to achieve reliable transmission and keep the information safe while improving data rates as well as confidentiality.

To cope with the above challenge, in this dissertation, a cooperative network technology is focused on, and the modern technologies to the emerging wireless scenarios is applied. In this paper, we will review these advanced schemes.

In order to achieve enhanced spectrum efficiency of the wireless mobile network, non orthogonalmultiple access (NOMA) has received attention by the researchers focusing on wireless systems [40–42]. Notably, different devices can share the same time and frequency spectrum with cooperative power allocation adjustment. Through the use of successive interference cancellation(SIC), the devices with weak power conditions can decode its own information after removing those strong power condition [43, 44], which has been investigated as an extension of the network-assisted interference cancellation and suppression (NAICS) in 3GPP [45, 46].

This technique significantly improve the spectral efficiency and outperform traditional orthogonal multiple access (OMA) schemes under the limitation of frequency spectrum. In Fig. 1, we illustrate the difference between OMA and NOMA. The OMA technique contains orthogonal frequency division multiple access (OFDMA) or time division multiple access (TDMA). In OFDMA, multiple devices are allocated with orthogonal subcarriers contacted via the orthogonal frequency-division multiplexing (OFDM) technique. In TDMA, the devices divide the signal into different time slots in order to share the same frequency channel. The downlink scenario with NOMA scheme is demonstrated in Fig. 1.2(a), where two devices (i.e., U1 and U2) receive information from a single base station (BS) with the same transmission channel. The BS continuously sends the signal to U1 and U2 simultaneously, where the two different signals are non-orthogonally superposed. In the decoding process, U1 needs to decode the signal of U2 and run SIC process of U2 signal before decoding its own signal.
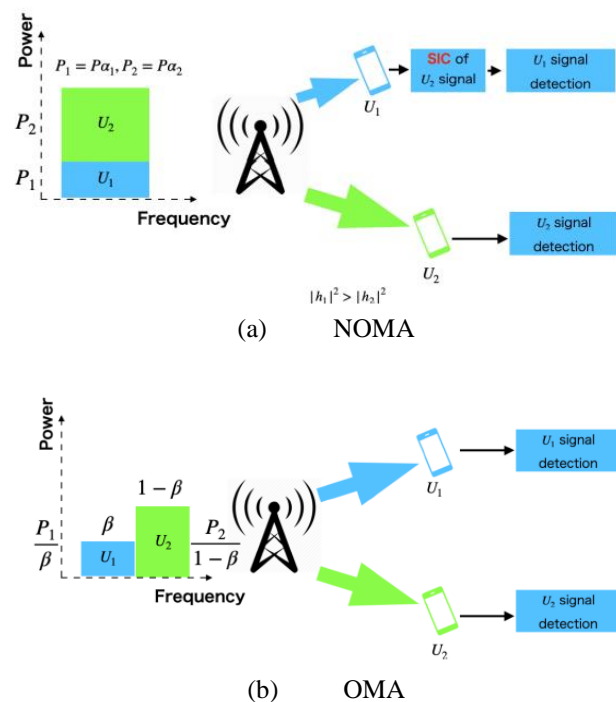

(a)   NOMA

(b)   OMA

Fig. 1: Multiple access scenarios for two devices that form a pair

II. SYSTEM MODEL

The system model of the NOMA-based cooperative relaying system is introduced in thispaper..We consider a simple cooperative relaying system (CRS) consisting of a source (S), decode-and-forward relay (R) which works in half-duplex mode, and a destination (D).We assume that all links between them (i.e., S-to-D, S to-R, and R-to-D) are available. The independent Rician fading channel coefficients of S-to-D, S-to-R, and R-to-D links are denoted as g_{SD}, g_{SR}, and g_{RD}, with the average powers of ω_{SD}, ω_{SR}, and ω_{RD}, respectively. It is also assumed that $\omega_{SD} < \omega_{SR}$, since in general the path loss of the S-to-D link is usually worse than that of the S-to-R link [10]. In the traditional CRS presented in Fig. 2(a), the source transmits X_1 to the relay and destination in the first time slot. Then in the second time slot, the relay transmits X_2 to the destination. In this way, the destination only receives one signal in two time slots. In the NOMA-based CRS showed in Fig. 2(b), the destination is able to receive two different signals in two time slots, so it outperforms the traditional CRS in terms of throughput. Specifically, in the first time slot, the source transmits the superposition of two different data symbols s1 and s2 to the relay and the destination as follows:

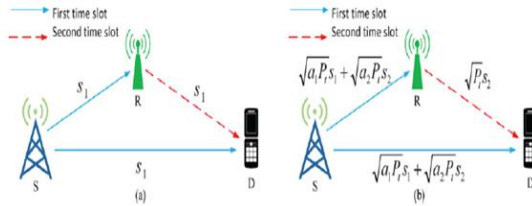Fig. 2. System models of two cooperative relaying systems:

(a) Traditional cooperative relaying systems;
(b) NOMA-based cooperative relaying systems.

$$y = \sqrt{a_1 W_t}\, x_1 + \sqrt{a_2 W_t}\, x_2 \tag{1}$$

where x_i denotes the i-th data symbol with normalized power $E[|x_i|^2] = 1$, W_t is the total transmit power, and a_i is the power allocation coefficient. It is noted that $a_1 + a_2 = 1$, and $a_1 > a_2$ due to $\Omega_{SD}^2 < \Omega_{SR}^2$ [5]. Thus, the received signals r_{SR} and r_{SD} at the relay and the destination in the first time slot are respectively expressed as

$$r_{SR} = h_{SR}\left(\sqrt{a_1 W_t}\, x_1 + \sqrt{a_2 W_t}\, x_2\right) + n_{SR} \tag{2}$$

$$r_{SD} = h_{SD}\left(\sqrt{a_1 W_t}\, x_1 + \sqrt{a_2 W_t}\, x_2\right) + n_{SD} \tag{3}$$

where n_{SR} and n_{SD} denote the additive white Gaussian noise (AWGN) with zero mean and variance σ^2. The destination only decodes symbol x_1 by treating symbol x_2 as noise, while the relay acquires symbol x_2 from (1) using SIC. Thus, the received signal-to-interference plus noise ratios (SINRs) for symbols x_1 and x_2 at the relay can be respectively obtained as

$$\gamma_{SR}^1 = \frac{|h_{SR}|^2 a_1 W_t}{|h_{SR}|^2 a_1 W_t + \sigma^2} \tag{4}$$

$$\gamma_{SR}^2 = \frac{|h_{SR}|^2 a_2 W_t}{\sigma^2} \tag{5}$$

and the received SINR for symbol x_1 at the destination is obtained as

$$\gamma_{SD} = \frac{|h_{SD}|^2 a_1 W_t}{|h_{SD}|^2 a_1 W_t + \sigma^2} \tag{6}$$

perfectly decode symbol x_2 in the first time slot [5], the received signal at the destination in the second time slot can be expressed as

$$r_{RD} = h_{RD}\sqrt{W_t}\, x_2 + n_{RD} \tag{7}$$

where n_{RD} is the AWGN with zero mean and variance σ^2, and the received SINR for symbol x_2 in (7) can be obtained as

$$\gamma_{RD} = \frac{|h_{RD}|^2 W_t}{\sigma^2} \tag{8}$$

As the expressions for received signals and SINRs are already acquired, we will calculate both the exact and approximated achievable rates in the NOMA-based CRS in the next section.

In this paper, we first derive the exact expression of the average achievable rate of the NOMA-based CRS over Rician fading channel. As the exact value of achievable rates are difficult to calculate, we further propose an approximation method using Gauss-Chebyshev Integration to simplify the numerical calculation.

Achievable Rate Analysis :

In this subsection, we analyze the average achievable rate of x_1 and x_2. Let $\lambda_{SD} \triangleq |h_{SD}|^2$, $\lambda_{SR} \triangleq |h_{SR}|^2$, $\lambda_{RD} \triangleq |h_{RD}|^2$ and $\triangleq P_t / \sigma^2$, where ρ represents the transmit SNR. As both the relay and the destination must successfully decode x_1 and x_2, the rates of these two signals should be lower than the rates of both links calculated by Shannon formula, so the achievable rate is the minimum of the rates of two different links. According to [10], we can obtain the achievable rates C_{x_1} and C_{x_2} of signals x_1 and x_2 respectively as

$$C_{x_1} = \frac{1}{2}\min\{\log_2(1+\gamma_{SD}), \log_2(1+\gamma_{SR}^1)\}$$
$$=$$
$$\frac{1}{2}\log_2(1+\min\{\lambda_{SD}, \lambda_{SR}\}\rho) - \frac{1}{2}\log_2(1+\min\{\lambda_{SD}, \lambda_{SR}\}\rho a_2) \tag{9}$$

$$C_{x_2} = \frac{1}{2}\min\{\log_2(1+\gamma_{SR}^2), \log_2(1+\gamma_{RD})\}$$

$$= \frac{1}{2}\log_2(1+\min\{a_2\lambda_{SR}, \lambda_{RD}\}\rho) \tag{10}$$

Let $z_1 \triangleq \min\{\lambda_{SD}, \lambda_{SR}\}$, $z_2 \triangleq \min\{a_2\lambda_{SR}, \lambda_{RD}\}\rho$. According to [11], we can get the cumulative distribution function (CDF) of z_1 as

$$F(z_1) = 1 - A_x A_y \sum_{k=0}^{\infty} \sum_{n=0}^{\infty} \check{B}_x(n) \check{B}_y(k) \Gamma(n+1, a_x z_1) \times$$
$$\Gamma(K+1, a_y z_1)$$

$$\overset{(a)}{\triangleq} 1 - A_x A_y \sum_{k=0}^{\infty} \sum_{n=0}^{\infty} \check{B}_x(n) \check{B}_y(k) n! \, k! \, e^{-(a_x + a_y) z_1} \times$$
$$\sum_{i=0}^{n} \sum_{j=0}^{k} \frac{a_x^i a_y^j}{i! j!} z_1^{i+j} \tag{11}$$

Where $\check{B}_x(n) = (K_x^n (1 + K_n)^n / (\Omega_x^n (n!))^2$, $\check{B}_y(K) = (K_x^n (1 + K_n)^n / (\Omega_y^k (K!))^2$, $a_x = (1 + K_x)/\Omega_x$, $a_y = (1 + K_y)/\Omega_y$, $A_x = a_x e^{-kx}$, $A_y = a_y e^{-ky}$, $\check{B}_x(n) = B_x(n)/a_x^{n+1}$, $\check{B}_y(k) = B_y(k)/a_y^{k+1}$. The subscript x denotes the S-to-D link, y denotes the S-to-R link, w denotes the R-to-D link, and K is the Rician factor. Note that the expansion form of incomplete Gamma function is used for the second equality (a) of (11).Then, we prove the convergence of the infinite summation in (11) as follows:

Proof: Let $P_x = (K_x(1 + K_x)/\Omega_x$, $Q_y = (K_y(1 + K_y)/\Omega_y$, we have

$$\frac{\Gamma(n+1, a_x z_1)}{n!} < \frac{\Gamma(n+1)}{n!} < 1, \tag{12}$$

$$\frac{\Gamma(k+1, a_y z_1)}{n!} < \frac{\Gamma(n+1)}{n!} < 1 , (3.13)$$

Then

$$= A_x A_y \sum_{k=0}^{\infty} \sum_{n=0}^{\infty} \check{B}_x(n) \check{B}_y(k) \Gamma(n+1, a_x z_1) \times$$
$$\Gamma(k+1, a_y z_1)$$

$$= A_x A_y \sum_{k=0}^{\infty} \sum_{n=0}^{\infty} \frac{P_x^n}{n!} \frac{Q_y^K}{k!} \frac{\Gamma(n+1, a_x z_1)}{n!} \frac{\Gamma(k+1, a_y z_1)}{k!}$$

$$< A_x A_y \sum_{k=0}^{\infty} \sum_{n=0}^{\infty} \frac{P_x^n}{n!} \frac{Q_y^K}{k!}$$

$$= A_x A_y e^{P_x + Q_y}$$

The final value will not change as k or n increases, so the infinite summation in (11) is convergent. Similarly, we can obtain the CDF of z_2 as follows:

$$G(z_2) = 1 - A_w A_y \sum_{n=0}^{\infty} \sum_{k=0}^{\infty} \check{B}_w(n) \check{B}_y(k) \Gamma(n+1, a_w z_2)$$
$$\times \Gamma(K+1, \frac{a_y}{a_2} z_2)$$

$$= 1 - A_w A_y \sum_{k=0}^{\infty} \sum_{n=0}^{\infty} \check{B}_w(n) \check{B}_y(k) n! \, k! \, e^{-(a_w + \frac{a_y}{a_2}) z_2} \times$$
$$\sum_{i=0}^{n} \sum_{j=0}^{k} \frac{a_w^i (\frac{a_y}{a_2})^j}{i! j!} z_2^{i+j} \tag{14}$$

where the parameters in (14) are similarly defined as those in (11).After the CDF of $z_1 \triangleq min\{\lambda_{SD}, \lambda_{SR}\}$ has been obtained as (11),we can substitute it into (9), and then the average achievable rate C_{x_1} of the signal x_1 as shown in (9) can be expressed as

$$C_{x_1} = \frac{1}{2} \int_0^{\infty} [log_2(1 + z_1 \rho) - log_2(1 + z_1 \rho a_2)] dF(z_1)$$

$$= \frac{1}{2 ln(2)} \left[\rho \int_0^{\infty} \frac{1 - F(z_1)}{1 + z_1 \rho} dz_1 - \rho a_2 \int_0^{\infty} \frac{1 - F(z_1)}{1 + z_1 \rho a_2} dz_1 \right] \tag{15}$$

Let $D(\rho) = \rho \int_0^{\infty} \frac{1 - F(z_1)}{1 + z_1 \rho} dz_1$, and and substitute (11) into $D(\rho)$, we have

$$D(\rho) = \rho \int_0^{\infty} \frac{1 - F(z_1)}{1 + z_1 \rho} dz_1$$

$$= A_x A_y \sum_{k=0}^{\infty} \sum_{n=0}^{\infty} \check{B}_x(n) \check{B}_y(k) n! \, k! \sum_{i=0}^{n} \sum_{j=0}^{k} \frac{a_x^i a_y^j}{i! j!} \times$$
$$\int_0^{\infty} \frac{z_1^{i+j} e^{-(a_x + a_y) z_1}}{1 + z_1 \rho} d(z_1 \rho)$$

$$\overset{(b)}{\triangleq} A_x A_y \sum_{k=0}^{\infty} \sum_{n=0}^{\infty} \check{B}_x(n) \check{B}_y(k) n! \, k! \sum_{i=0}^{n} \sum_{j=0}^{k} \frac{a_x^i a_y^j}{i! j! \rho^{i+j}} \times$$
$$\int_0^{\infty} \frac{t^{i+j} e^{\frac{-(a_x + a_y) z_1}{\rho}}}{1 + t} d(t) \tag{16}$$

Where (b) is obtained by setting $t = z_1 \rho$
Now we have the following Lemma 1 to calculate the integral

$$\int_0^{\infty} \frac{t^{i+j} e^{\frac{-(a_x + a_y) z_1}{\rho}}}{1 + t} d(t) \text{ in (16)}$$

Lemma 1: For $m \in \mathbb{Z}^*$ and $\beta > 0$, we have

$$\int_0^{\infty} \frac{t^m e^{-\beta t}}{1 + t} d(t) = e^{\beta} m! \Gamma(-m, \beta), \tag{17}$$

Where

$$\Gamma(-m, \beta) =$$
$$\int_\beta^\infty \frac{e^{-t}}{t^{m+1}} dt \text{ denotes the incomplete Gamma function.}$$

Proof: Let $x = \beta(1 + t)$, we have

$$\int_0^\infty \frac{t^m e^{-\beta t}}{1+t} d(t) = \frac{e^\beta}{\beta^m} \int_\beta^\infty \frac{(x-\beta)^m e^{-x}}{x} dx \qquad (18)$$

Then we define :

$$J_m(x) = \frac{(x-\beta)^m}{x}, \qquad (19)$$

$$I(x) = \frac{e^\beta}{\beta^m} \int_\beta^\infty J_m(x) e^{-x} dx \qquad (20)$$

On the one hand, by substituting (19) into (20), we have

$$I(x) = -\frac{e^\beta}{\beta^m} \int_\beta^\infty \frac{(x-\beta)^m e^{-x}}{x} d(e^{-x})$$

$$= -\frac{e^\beta}{\beta^m} \frac{(x-\beta)^m e^{-x}}{x}\Big|_\beta^\infty + \frac{e^\beta}{\beta^m} \int_\beta^\infty \frac{(x-\beta)^{m-1}(mx-x-\beta)}{x^2} e^{-x} d(x)$$

$$= \frac{e^\beta}{\beta^m} \int_\beta^\infty J_{m-1}(x) e^{-x} dx \qquad (21)$$

We can observe from (21) that as long as β is a root of $J_m(x)$,the integral can be successively calculated by using (21) for m times. On the other hand, we know that $J_m(x) = \frac{(x-\beta)^m}{x} = x^{m-1} + a_{m-2} x^{m-2} + \dots + a_0 + (-1)^m \beta^m / x$, so after m times of integration by part, we will have

$$I(x) = -\frac{e^\beta}{\beta^m} \int_\beta^\infty \frac{(x-\beta)^m e^{-x}}{x} d(e^{-x})$$

$$I(x) = -\frac{e^\beta}{\beta^m} \int_\beta^\infty \left(x^{m-1} + \dots + a_0 + (-1)^m \frac{\beta^m}{x}\right)^{(m)} d(e^{-x})$$

$$I(x) = -\frac{e^\beta}{\beta^m} \int_\beta^\infty \left((-1)^m \frac{\beta^m}{x}\right)^{(m)} d(e^{-x})$$

$$= e^\beta m! \Gamma(-m, \beta), \qquad (22)$$

where $(\cdot)^{(m)}$ denotes m-order derivation. Substitute (17) in Lemma 1 into (16), we can get the final exact expression of C_{x_1} as

$$C_{x_1} = \frac{1}{2\ln(2)} (D(\rho) - D(\rho a_2)), \qquad (23)$$

Where

$$= A_x A_y \sum_{k=0}^\infty \sum_{n=0}^\infty \check{B}_x(n) \check{B}_y(k) n! k! \times$$
$$\sum_{i=0}^n \sum_{j=0}^k \frac{(i+j)! a_x^i a_y^j}{i! j! \rho^{i+j}} e^{\frac{-(a_x+a_y)}{\rho}} \Gamma\left(-i-j, \frac{(a_x+a_y)}{\rho}\right), \qquad (24)$$

and $D(\rho a_2)$ shares the same form as $D(\rho)$. Similarly, we can derive the exact expression of C_{x_2} as

$$C_{x_2} = \frac{1}{2\ln(2)} A_x A_y \sum_{k=0}^\infty \sum_{n=0}^\infty \check{B}_x(n) \check{B}_y(k) n! k! \times$$
$$\sum_{i=0}^n \sum_{j=0}^k \frac{(i+j)! a_w^i (\frac{a_y}{a_2})^j}{i! j! \rho^{i+j}} e^{\frac{-(a_w + \frac{a_y}{a_2})}{\rho}} \Gamma\left(-i-j, \frac{(a_w + \frac{u_y}{a_2})}{\rho}\right), \qquad (25)$$

Although we have derived the exact expressions of the achievable rates of x1 and x2 in (23) and (25) respectively, such expressions are very complicated, since the incomplete Gamma function is difficult to calculate. Thus, it is still difficult to get the exact values of the achievable rates, which motivates us to propose an approximation method to solve this problem in the next subsection.

Achievable Rate Approximation:

In this subsection, we propose an approximation method using Gauss-Chebyshev Integration [12] to simplify the numerical calculation of the incomplete Gamma function $\Gamma(-m, \beta)$. However, Gauss-Chebyshev Integration is used on the limited interval $[-1, 1]$, while the integral intervals in incomplete Gamma functions of (23) and (25) are infinite intervals. Thus, we set $t = 2\beta \frac{1}{x} - 1$ and convert the incomplete Gamma function as

$$\Gamma(-m, \beta) = \left(\frac{1}{2\beta}\right)^m \int_{-1}^1 \frac{1}{\sqrt{1-t^2}} (t+1)^{m-1} e^{\frac{-2\beta}{t+1}} \sqrt{1-t^2} \, dt$$

$$= \left(\frac{1}{2\beta}\right)^m \frac{\pi}{n} \sum_{i=1}^n \left(\cos\left(\frac{2l-1}{2n}\pi\right) + 1\right)^{m-1} \times$$
$$e^{-\frac{2\beta}{\cos\left(\frac{2l-1}{2n}\pi\right)+1}} \left|\sin\left(\frac{2l-1}{2n}\pi\right)\right| \qquad (26)$$

where n is the approximation order. Substituting (26) into the exact expression of the achievable rate (23), we can finally obtain the approximation of (23) as

$$C_{x_1} = \frac{1}{2\ln(2)}(D(\rho) - D(\rho a_2)), \quad (27)$$

where

$$D(\rho) = A_x A_y \sum_{k=0}^{\infty} \sum_{n=0}^{\infty} \tilde{B}_x(n) \tilde{B}_y(k) n! \, k! \times$$

$$\sum_{i=0}^{n} \sum_{j=0}^{k} \frac{(i+j)! a_x^i a_y^j}{i! j! \rho^{i+j}} \times e^{\frac{-(a_x+a_y)}{\rho}} \left(\frac{1}{2^{\frac{(a_x+a_y)}{\rho}}}\right)^{i+j} \frac{\pi}{n} \sum_{l=1}^{n} \left(\cos\left(\frac{2l-1}{2n}\pi\right) + \right.$$

$$\left. 1\right)^{i+j-1} \times e^{-\frac{2^{\frac{(a_x+a_y)}{\rho}}}{\cos\left(\frac{2l-1}{2n}\pi\right)+1}} \left|\sin\left(\frac{2l-1}{2n}\pi\right)\right|, \quad (28)$$

and $D(\rho a_2)$ shares the same form as $D(\rho)$.
Similarly, (25) can be approximated as

$$C_{x_2} = \frac{1}{2\ln(2)} A_x A_y \sum_{k=0}^{\infty} \sum_{n=0}^{\infty} \tilde{B}_x(n) \tilde{B}_y(k) n! \, k! \times$$

$$\sum_{i=0}^{n} \sum_{j=0}^{k} \frac{(i+j)! a_w^i (\frac{a_y}{a_2})^j}{i! j! \rho^{i+j}} \times e^{\frac{(a_x+\frac{a_y}{a_2})}{\rho}} \left(\frac{1}{2^{\frac{(a_w+\frac{a_y}{a_2})}{\rho}}}\right)^{i+j} \frac{\pi}{n} \sum_{l=1}^{n} \left(\cos\left(\frac{2l-1}{2n}\pi\right) + \right.$$

$$\left. 1\right)^{i+j-1} \times e^{-\frac{2^{\frac{(a_w+\frac{a_y}{a_2})}{\rho}}}{\cos\left(\frac{2l-1}{2n}\pi\right)+1}} \left|\sin\left(\frac{2l-1}{2n}\pi\right)\right|, \quad (29)$$

Thus, the approximated achievable rates (27) and (29) can be conveniently calculated numerically, and their accuracy will be validated by the simulation results in the next paper.

III. RESULT

In this paper, we compare the analytical results obtained in the this paper with Monte Carlo simulations to validate their accuracy. Specifically, 10^5 realizations of Rician distribution random variables are generated, and the approximation order for Gauss-Chebyshev Integration is set as 100.
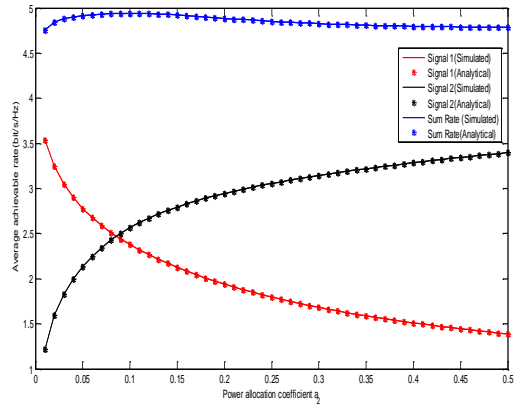

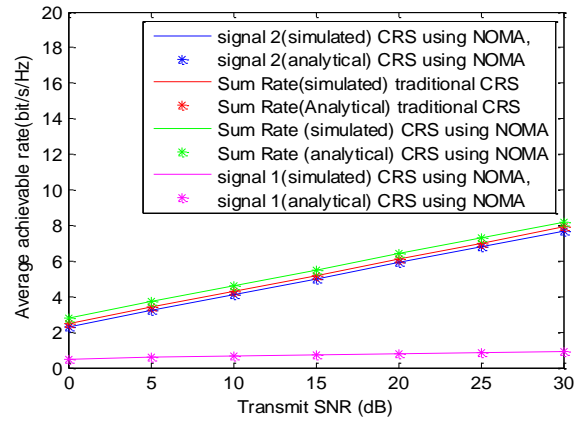**Fig.3.** Achievable rates for the NOMA-based CRS over Rician fadingchannels.

Fig. 4. Achievable rates comparison between the NOMA based CRS and traditional CRS

Fig. 3 presents the achievable rate performance of s1, s2 and the corresponding sum rate of the NOMA-based CRS against the power allocation coefficient a_2. In the model of Rician fading channel, the parameter Ω denotes the average power gain of the channel [13], which is usually determined by distances between transceivers. In our system , Ω_i ($i \in \{SD, SR, RD\}$) denotes the average power gain of link SD, link SR, and link RD, mainly reflecting the impacts of distances

from S to D, from S to R, and from R to D, respectively. Thus, we set $\Omega_{SD} = 9 < \Omega_{SR} = \Omega_{RD} = 36$ [10], because the distances from S to R and from R to D are usually smaller than the distance from S to D, and thus link SR and link RD have higher average power gains than link SD. According to [11], other parameters are set as SNR = 20 dB, $K_{SR} = K_{RD} = 5$, and $K_{SD} = 2$. From Fig. 3, we can observe that the derived analytical results using Gauss-Chebyshev Integration match well with the simulation results. In addition, as a_2 increases, s2 will get more power and its achievable rate increases accordingly, while the achievable rate of *s1*

decreases. Moreover, the sum rate of two signals first increases and then slowly decreases with the increase of a_2. Actually, we can see from (10) that when a_2 is small, the achievable rate of s_2 is mainly determined by link SR, as $a_2\lambda_{SR}$ will always be smaller than λ_{RD} . Due to SIC, s_2 will have no interference in link SR, so increasing a_2 will largely increase the achievable rate of s_2, and thus increase the sum rate. However, when a_2 increases, $a_2\lambda_{SR}$ will be larger than λ_{RD} at last, and the rate of link RD will slowly become the determinant factor, which is not influenced by a_2.As a result, the increase of s_2 achievable rate finally cannot make up for the decrease of s_1's achievable rate, which causes the decrease of the sum rate, as shown in Fig. 3. Thus, there exists an optimal power allocation coefficient to maximize the sum rate, which is an interesting research topic deserving further investigation in the future. Fig. 4 compares the achievable rates of the traditional CRS and the NOMA-based CRS against the transmit SNR, where we set $a_2 = 0.4, \Omega_{SD} = 9, \Omega_{RD} = 36$, and $\Omega_{SR} = 144$. We find that the simulation results and analytical results are consistent, and the NOMA-based CRS achieves higher achievable sum rate than the traditional CRS, since NOMA-based CRS can transmit two signals in two slots, while traditional CRS can only transmit one signal during the same time.

V. CONCLUSION

In this paper, we have investigated the performance of a NOMA based cooperative relaying system by deriving the exact analytical expressions of the achievable rates. Moreover, an efficient approximation method using Gauss-Chebyshev Integration for the achievable rates was also proposed, which enables the sum series of the achievable rate expressions converge quickly. Simulation results have verified that our derived analytical results match well with the Monte Carlo simulations, and the NOMA-based CRS is able to achieve higher achievable rate than the traditional CRS.

REFERENCES

[1] K. J. R. Liu, A. K. Sadek,W. Su, and A. Kwasinski, Cooperative Communications and Networking. New York City, NY, USA: Cambridge University Press, 2009.

[2] P. N. Son and H. Y. Kong, "Cooperative communication with energy-harvesting relays under physical layer security," IET Commun., vol. 9, no. 17, pp. 2131–2139, Nov. 2015.

[3] R. Fan, J. Cui, S. Jin, K. Yang, and J. An, "Optimal node placement and resource allocation for UAV relaying network," IEEE Commun. Lett., vol. 22, no. 4, pp. 808–811, Apr. 2018.

[4] M. Ju and H.-C. Yang, "Optimum design of energy harvesting relay for two-way decode-and forward relay networks under max-min and max-sum criterions," IEEE Trans. Commun., vol. 67, no. 10, pp. 6682–6697, Oct. 2019.

[5] K. Sultan, "Best relay selection schemes for NOMA based cognitive relay networks in underlay spectrum sharing," IEEE Access, vol. 8, pp. 190 160–190 172, 2020.

[6] A. Sendonaris, E. Erkip, and B. Aazhang, "User cooperation diversity-part I: System description,"IEEE Trans. Commun., vol. 51, no. 11, pp. 1927–1938, Nov. 2003.

[7] "User cooperation diversity-part II: Implementation aspects and performance analysis," IEEE Trans. Commun., vol. 51, no. 11, pp. 1939–1948, Nov. 2003.

[8] R. U. Nabar, H. Bolcskei, and F. W. Kneubuhler, "Fading relay channels: Performance limits and space-time signal design," IEEE J. Sel. Areas Commun., vol. 22, no. 6, pp. 1099–1109, Aug. 2004.

[9] H. Cui, L. Song, and B. Jiao, "Multi-pair two-way amplify-and-forward relaying with very large number of relay antennas," IEEE Trans. Wireless Commun., vol. 13, no. 5, pp. 2636–2645, May 2014.

[10] S. Luo and K. C. Teh, "Amplify-and-forward based two-way relay arq system with relay combination,"IEEE Commun. Lett., vol. 19, no. 2, pp. 299–302, Feb. 2015.

[11] D. Li, "Amplify-and-forward relay sharing for both primary and cognitive users," IEEE Trans. Veh.Technol., vol. 65, no. 4, pp. 2796–2801, Apr. 2016.

[12] Y. Dong, M. J. Hossain, and J. Cheng, "Performance of wireless powered amplify and forward relaying over Nakagami-mfading channels with nonlinear energy harvester," IEEE Commun. Lett.,vol. 20, no. 4, pp. 672–675, Apr. 2016.

[13] S. Li, K. Yang, M. Zhou, J. Wu, L. Song, Y. Li, and H. Li, "Full-duplex amplify-and-forward relaying: Power and location optimization," IEEE Trans. Veh. Technol., vol. 66, no. 9, pp. 8458– 8468, Sep. 2017.

[14] K. M. Rabie and B. Adebisi, "Enhanced amplify-and-forward relaying in non-Gaussian PLC networks,"IEEE Access, vol. 5, pp. 4087–4094, 2017.

[15] L. Jiang and H. Jafarkhani, "mmWave amplify-and-forward MIMO relay networks with hybrid precoding/combining design," IEEE Trans. Wireless Commun., vol. 19, no. 2, pp. 1333–1346, Feb. 2020.

[16] A. S. Ibrahim, A. K. Sadek, W. Su, and K. J. R. Liu, "Cooperative communications with relay selection:When to cooperate and whom to cooperate with?" IEEE Trans. Wireless Commun., vol. 7, no. 7, pp. 2814–2827, Jul. 2008.

[17] M. R. Bhatnagar, R. K. Mallik, and O. Tirkkonen, "Performance evalution of best-path selection in a multihop decode-and-forward cooperative system," IEEE Trans. Veh. Technol., vol. 65, no. 4, pp.2722–2728, Apr. 2016.

[18] Y. Gu and S. Aissa, "RF-based energy harvesting in decode-and-forward relaying systems: Ergodic and outage capacities," IEEE Trans. Wireless Commun., vol. 14, no. 11, pp. 6425–6434, Nov. 2015.

[19] G. T. Djordjevic, K. Kansanen, and A. M. Cvetkovic, "Outage performance of decode-and-forward cooperative networks over Nakagami-m fading with node blockage," IEEE Trans. Wireless Commun.,vol. 15, no. 9, pp. 5848–5860, Sep. 2016.

[20] H. Liu, Z. Ding, K. J. Kim, K. S. Kwak, and H. V. Poor, "Decode-and-forward relaying for cooperative NOMA systems with direct links," IEEE Trans. Wireless Commun., vol. 17, no. 12, pp.8077–8093, Dec. 2018.

[21] R. Fan, S. Atapattu, W. Chen, Y. Zhang, and J. Evans, "Throughput maximization for multihop decode-and-forward relay network with wireless energy harvesting," IEEE Access, vol. 6, pp.24 582–24 595, 2018.

[22] O. M. Kandelusy and S. M. H. Andargoli, "Outage performance of decode-and-forward (DF)-based multiuser spectrum sharing relay system with direct link in the presence of primary users' power,"IET Commun., vol. 12, no. 3, pp. 246–254, Feb. 2018.

[23] E. Li, X. Wang, Z. Wu, S. Hao, and Y. Dong, "Outage analysis of decode-and-forward two-way relay selection with different coding and decoding schemes," IEEE Syst. J., vol. 13, no. 1, pp.125–136, Mar. 2019.

[24] M. Asadpour, B. Van den Bergh, D. Giustiniano, K. A. Hummel, S. Pollin, and B. Plattner, "Micro aerial vehicle networks: an experimental analysis of challenges and opportunities," IEEE Commun.Mag., vol. 52, no. 7, pp. 141–149, Jul. 2014.

[25] K. Namuduri, S. Chaumette, J. H. Kim, and J. P. G. Sterbenz, UAV Networks and Communications. Cambridge University Press, 2017.

[26] K. P. Valavanis and G. J. Vachtsevanos, Handbook of Unmanned Aerial Vehicles. Springer, 2015.

[27] F. Ono, H. Ochiai, and R. Miura, "A wireless relay network based on unmanned aircraft system with rate optimization," IEEE Trans. Wireless Commun., vol. 15, no. 11, pp. 7699–7708, Nov. 2016.

[28] M. M. Azari, F. Rosas, K.-C. Chen, and S. Pollin, "Ultra reliable UAV communication using altitude and cooperation diversity," IEEE Trans. Commun., vol. 66, no. 1, pp. 330–344, Jan. 2018.

[29] M. M. Azari, F. Rosas, and P. Sofie, "Cellular connectivity for UAVs: Network modeling, performance

[30] W. Wang, X. Li, M. Zhang, K. Cumannan, D. W. K. Ng, G. Zhang, J. Tang, and O. A. Dober, "Energy-constrained UAV-assisted secure communications with position optimization and cooperative jamming," IEEE Trans. Commun., vol. 68, no. 7, pp. 4476–4489, Jul. 2020.

[31] H. Shakhatreh, A. H. Sawalmeh, A. Al-Fuqaha, Z. Dou, E. Almaita, I. Khalil, N. S. Othman,A. Khreishah, and M. Guizani, "Unmanned aerial vehicles (UAVs): A survey on civil applications and key research challenges," IEEE Access, vol. 7, pp. 48 572–48 634, 2019.

[32] W. Ejaz, M. A. Azam, S. Saadat, F. Iqbal, and A. Hanan, "Unmanned aerial vehicle enabled IoT platform for disaster management," Energies, vol. 12, no. 14, p. 2706, Jul. 2019.

[33] Y. Zeng, R. Zhang, and T. J. Lim, "Wireless communications with unmanned aerial vehicles: opportunities and challenges," IEEE Commun. Mag., vol. 54, no. 5, pp. 36–42, May 2016.

[34] J. Zhao, F. Gao, Q. Wu, S. Jin, Y. Wu, and W. Jia, "Beam tracking for UAV mounted Sat Com on the-move with massive antenna array," IEEE J. Sel. Areas Commun., vol. 36, no. 2, pp. 363–375,Feb. 2018.

[35] Y. Zeng, R. Zhang, and T. J. Lim, "Throughput maximization for UAV-enabled mobile relaying systems," IEEE Trans. Commun., vol. 64, no. 12, pp. 4983–4996, Dec. 2016.

[36] Y. Zhang, Z. Mou, F. Gao, L. Xing, J. Jiang, and Z. Han, "Hierarchical deep reinforcement learning for backscattering data collection with multiple UAVs," IEEE Internet Things J., vol. 8, no. 5, pp.3786–3800, Mar. 2021.

[37] J. Zhao, Y. Wang, Z. Fei, X. Wang, and Z. Miao, "NOMA-aided UAV data collection system: Trajectory optimization and communication design," IEEE Access, vol. 8, pp. 155 843–155 858,2020.

[38] F. Luo, C. Jiang, J. Du, J. Yuan, Y. Ren, S. Yu, and M. Guizani, "A distributed gateway selection algorithm for UAV networks," IEEE Trans. Emerg. Topics Comput., vol. 3, no. 1, Mar. 2015.

[39] R. Duan, J. Wang, C. Jiang, Y. Ren, and L. Hanzo, "The transmit-energy vs computation-delay trade-off in gateway-selection for heterogenous cloud aided multi-UAV systems," IEEE Trans.Commun., vol. 67, no. 4, pp. 3026–3039, Apr. 2019.

[40] M. Vaezi, R. Schober, Z. Ding, and H. V. Poor, "Non-orthogonal multiple access: Common myths and critical questions," IEEE Wireless Commun., vol. 26, no. 5, pp. 174–180, Oct. 2019.

[41] M. Vaezi and H. V. Poor, "NOMA: An information-theoretic perspective," in Multiple Access Techniques for

5G Wireless Networks and Beyond, M. Vaezi, Z. Ding, and H. V. Poor, Eds. Cham:Springer International Publishing, 2019, pp. 167–193.

[42] F. Mokhtari, M. R. Milli, F. Eslami, F. Ashtiani, B. Makki, M. Mirmohseni, M. Nasiri-Kenari, and T. Svensson, "Download elastic traffic rate optimization via NOMA protocols," IEEE Trans. Veh. Technol., vol. 68, no. 1, pp. 713–727, Jan. 2019.

[43] Z. Ding, M. Peng, and H. V. Poor, "Cooperative non-orthogonal multiple access in 5G systems,"IEEE Commun. Lett., vol. 19, no. 8, pp. 1462–1465, Aug. 2015.

[44] S. M. R. Islam, N. Avazov, O. A. Dobre, and K.-s. Kwak, "Power-domain non-orthogonal multiple access (NOMA) in 5G systems: Potentials and challenges," IEEE Commun. Surveys Tuts., vol. 19, no. 2, pp. 721–742, Second quarter 2017.

[45] 3GPP, "Study on network-assisted interference cancellation and suppression (NAICS) for LTE v.12.0.1," 3rd Generation Partnership Project (3GPP), Sophia Antipolis, France, Rep. TR 36.866, Mar. 2014.

[46] Media Tek, "Study on downlink multiuser superposition transmission (MUST) for LTE," 3rd Generation Partnership Project (3GPP), Hsinchu, Taiwan, Rep. TR 36.859, Apr. 2015.

[47] B. Wu, J. Chen, J. Wu, and M. Cardei, "A survey of attacks and countermeasures in mobile ad hoc networks," in Wireless Network Security, Y. Xiao, X. S. Shen, and D.-Z. Du, Eds. Boston, MA,USA: Springer, 2007, ch. 5, pp. 103–135.

[48] Y. Wang, G. Attebury, and B. Ramamurthy, "A survey of security issues in wireless sensor networks,"IEEE Commun. Surveys Tuts., vol. 8, no. 2, pp. 2–23, Second Quarter 2006.

[49] T. T. Karygiannis and L. Owens, "Wireless network security: 802.11, bluetooth and handheld devices," Gaithersburg, MD, USA, Nov. 2002.

[50] P. W. Shor, "Algorithms for quantum computation: discrete logarithms and factoring," in Proc.IEEE Annu. Symp. Found. of Comput. Sci. (FOCS), Santa Fe, NM, USA, Nov. 1994.

[51] R. K. Nichols and P. C. Lekkas, Wireless Security: Models, Threats, and Solutions. New York,NY, USA: McGraw-Hill, 2002.

[52] M. Bloch and J. Barros, Physical-Layer Security: From Information Theory to Security Engineering.Cambridge, United Kingdom: Cambridge University Press, 2011.

[53] A. D. Wyner, "The wire-tap channel," Bell Syst. Tech. J., vol. 54, no. 8, pp. 1355–1387, 1975.